# Pole position of the $a_1(1260)$

Misha Mikhasenko

Joint Physics Analysis Center,
COMPASS @ CERN,
Universität Bonn, HISKP, Bonn, Germany

CHARM 2018
Akademgorodok, Novosibirsk

23/05/2018


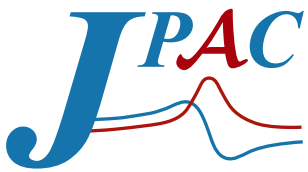


Bundesministerium
für Bildung
und Forschung

# Overview

# Flavor and excitation

## Quark model

- color-binding,

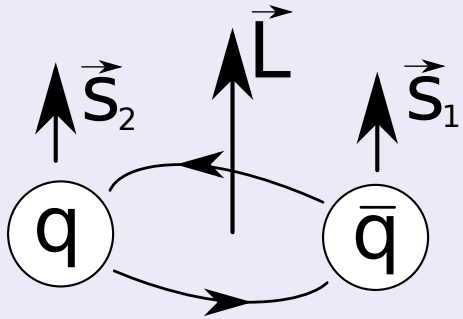


  - Radial excitation ($n$),
  - Orbital excitation ($L$),

- many states ($J^{PC} = 0^{++}, 1^{--} \ldots$) are coupled to $\pi\pi$.
- Some other to $3\pi$ system

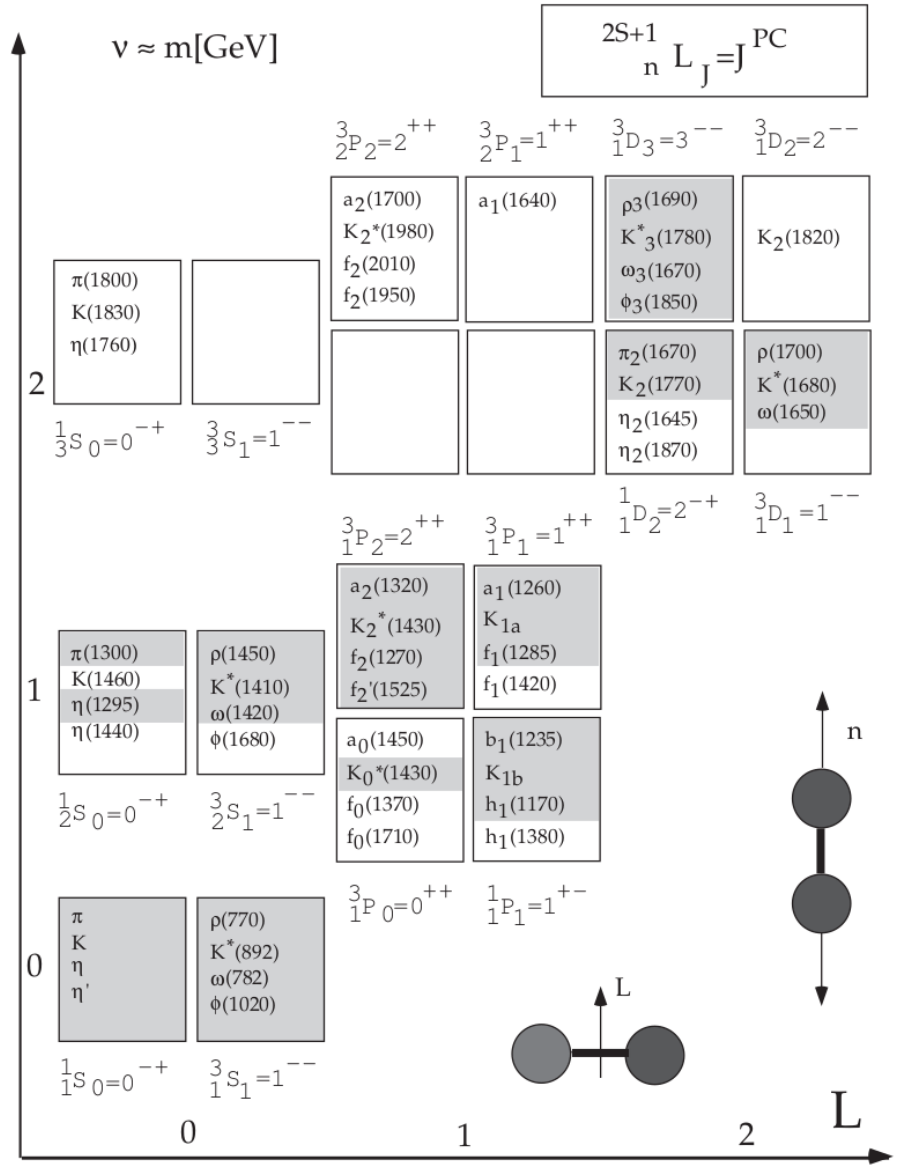


[Amsler et al., Phys. Rept. 389, 61 (2004)]

# Lattice QCD

## Lattice QCD spectrum matches experimental observations well but predicts more

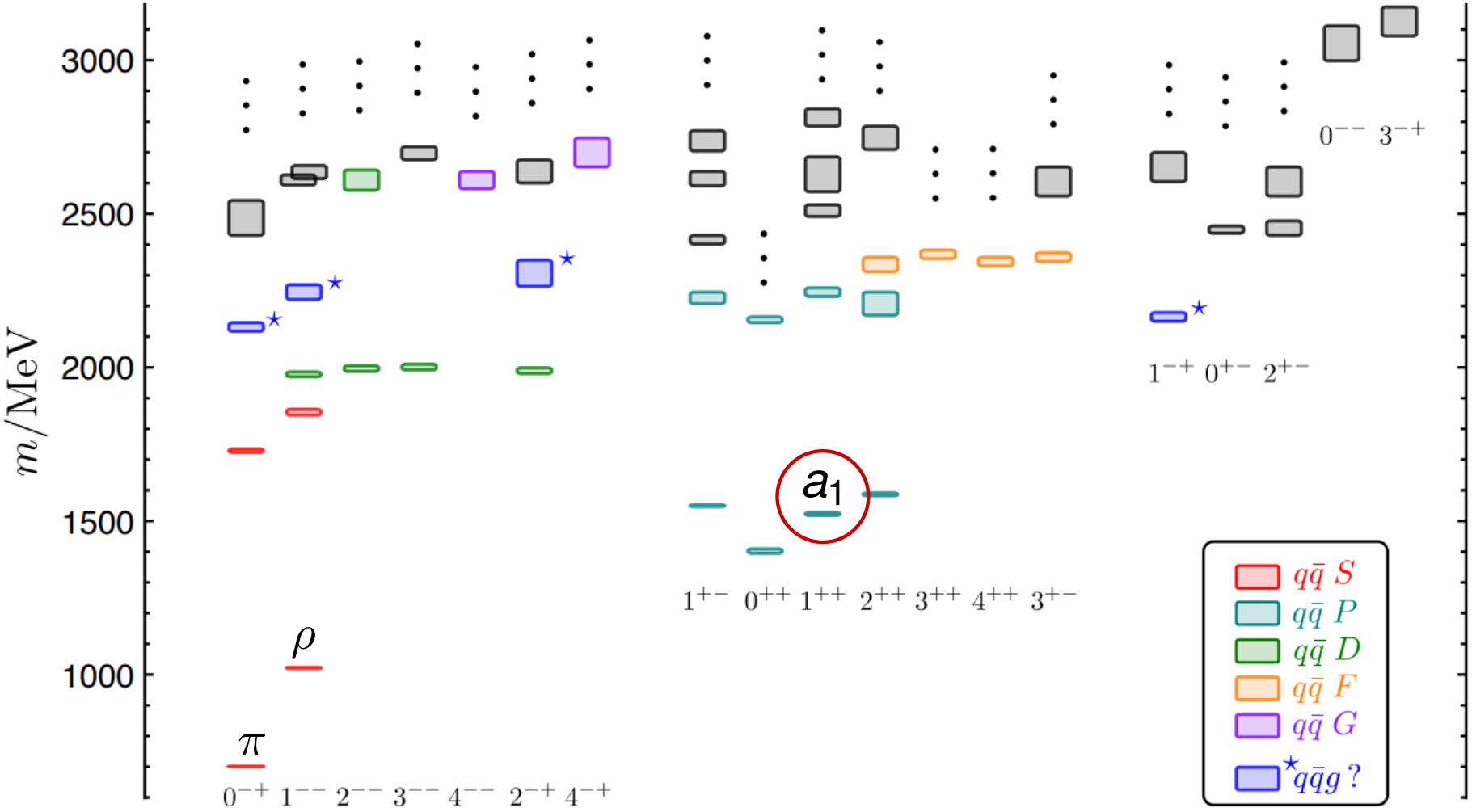


[Dudek et. al, Phys.Rev. D82 (2010) 034508]

# Resonances on the Lattice

## $\pi\pi$ system in the box

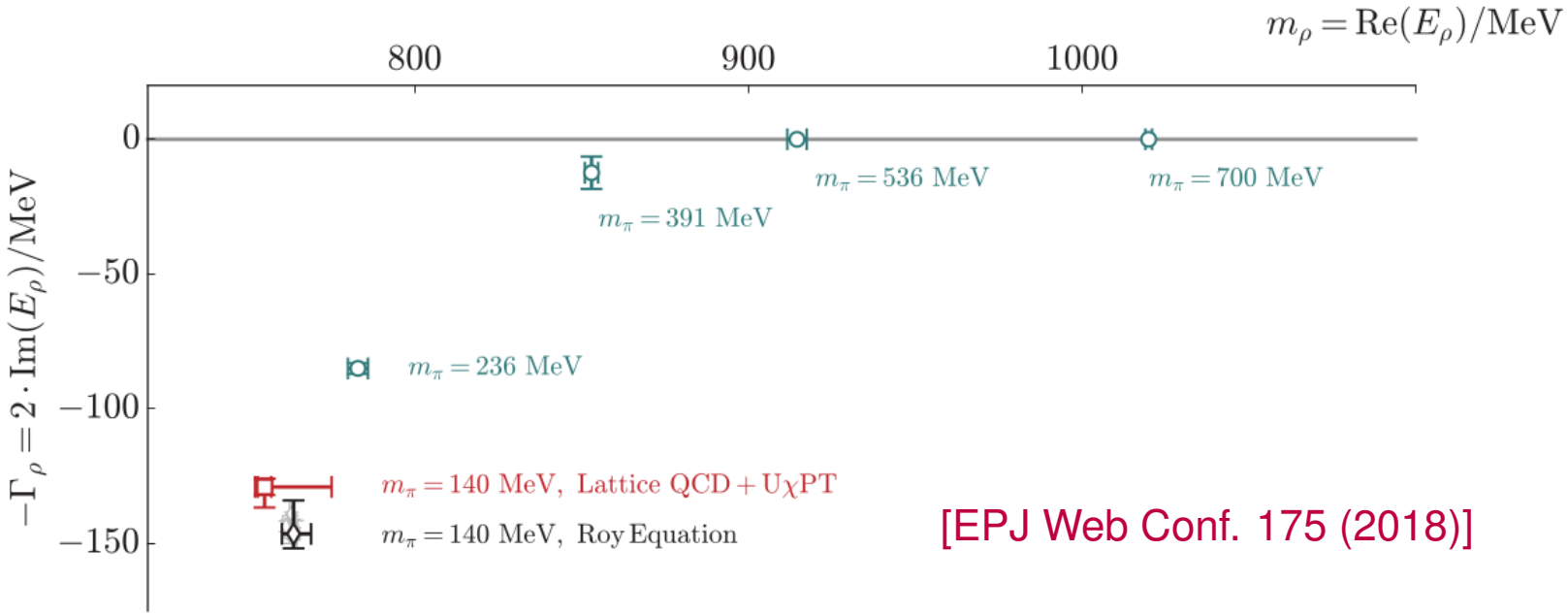


[EPJ Web Conf. 175 (2018)]

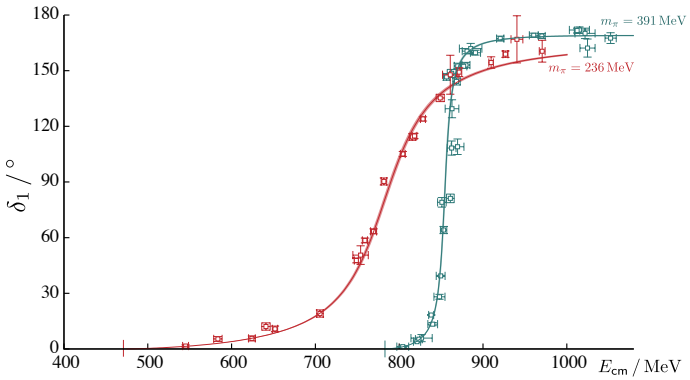


[Wilson, D. et al.,PRD 92,(2015)]

## Tracking pole position

- For high $m_\pi$ the $\rho$-becomes stable. Pole of $\rho$ approaches real axis.

# Resonances = Poles at the Complex plane

## Breit-Wigner amplitude

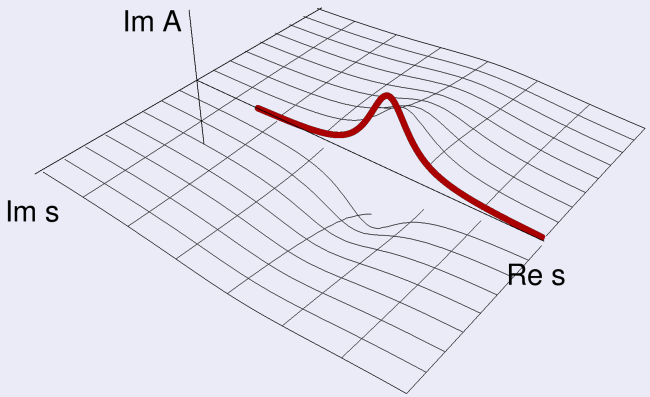


Features of the complex $s$ plane:

- $s = E^2$ – the total inv.mass squared
- The Real axis $\rightarrow$ physical world
- The Imaginary axis $\rightarrow$ analytical continuation

# Resonances = Poles at the Complex plane

## Breit-Wigner amplitude

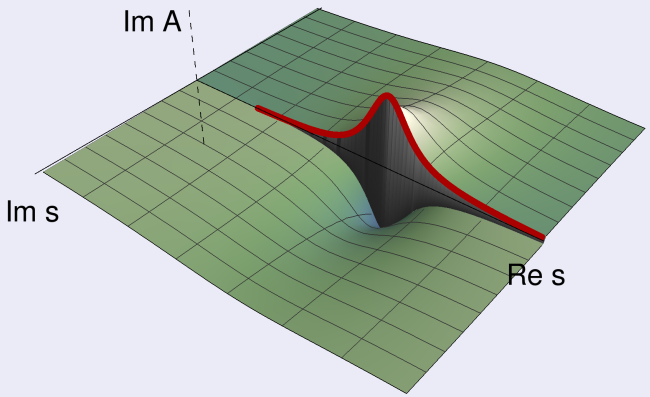


Features of the complex $s$ plane:

- $s = E^2$ – the total inv.mass squared
- The Real axis $\rightarrow$ physical world
- The Imaginary axis $\rightarrow$ analytical continuation

# Resonances = Poles at the Complex plane

## Breit-Wigner amplitude

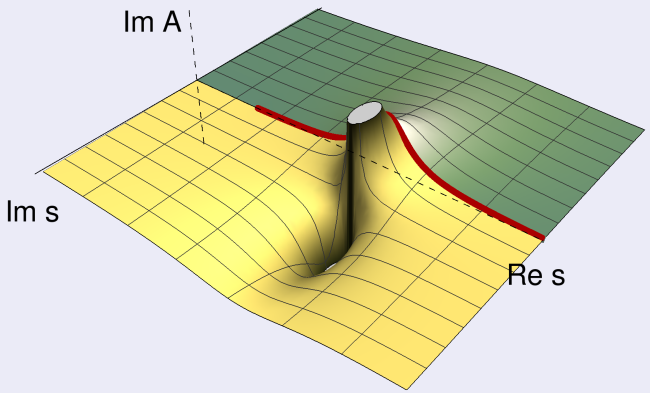


Features of the complex $s$ plane:

- $s = E^2$ – the total inv.mass squared
- The Real axis $\rightarrow$ physical world
- The Imaginary axis $\rightarrow$ analytical continuation

## Unitarity constaints for **two-body** scattering

- $\hat{S}^\dagger \hat{S} = \hat{\mathbb{I}} \quad \hat{S} = \hat{\mathbb{I}} + i\hat{T}$ $\qquad \hat{T} - \hat{T}^\dagger = i\hat{T}^\dagger \hat{T}.$
- $T(s,t) = \left\langle p_1' p_2' | \hat{T} | p_1 p_2 \right\rangle$ $\qquad 2\mathrm{Im}\, T(s,t) = \int \mathrm{d}\Phi_2\, T^*(s,t')\, T(s,t'')$
- Partial wave expansion $\longrightarrow$
- The final form $\qquad 2\mathrm{Im}\, t_l(s) = t_l^*(s)\rho(s)t_l(s)$

# Resonances = Poles at the Complex plane

## Breit-Wigner amplitude

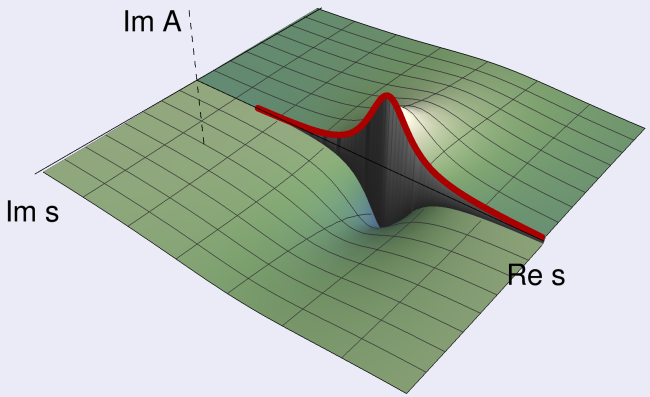


Features of the complex $s$ plane:

- $s = E^2$ – the total inv.mass squared
- The Real axis $\rightarrow$ physical world
- The Imaginary axis $\rightarrow$ analytical continuation

## Unitarity constaints for **two-body** scattering

- $\hat{S}^\dagger \hat{S} = \hat{\mathbb{I}} \quad \hat{S} = \hat{\mathbb{I}} + i\hat{T}$ $\qquad \hat{T} - \hat{T}^\dagger = i\hat{T}^\dagger \hat{T}.$
- $T(s,t) = \left\langle p_1' p_2' | \hat{T} | p_1 p_2 \right\rangle$ $\qquad 2\mathrm{Im}\, T(s,t) = \int \mathrm{d}\Phi_2\, T^*(s,t')\, T(s,t'')$
- Partial wave expansion $\longrightarrow$
- The final form $\qquad 2\mathrm{Im}\, t_l(s) = t_l^*(s)\rho(s)t_l(s)$

# Quasi-two-body unitarity

[MM (JPAC) in preparation]

## **Three-body** unitarity

[Eden, Landshoff et al.(2002)]

- Singularity splitting:
- Final state interaction:

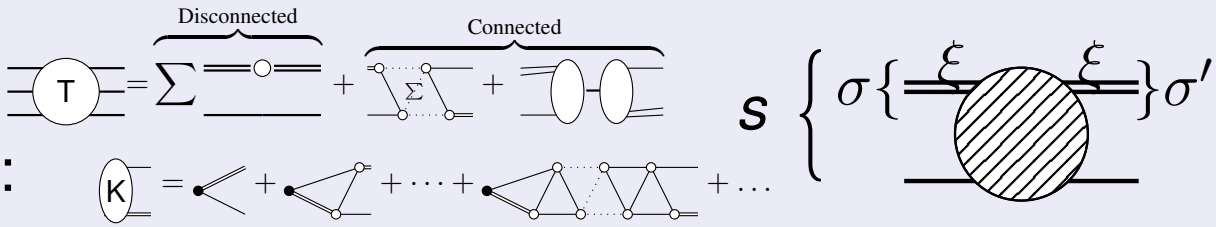

# Quasi-two-body unitarity

[MM (JPAC) in preparation]

## **Three-body** unitarity

[Eden, Landshoff et al.(2002)]

- Singularity splitting:
- Final state interaction:

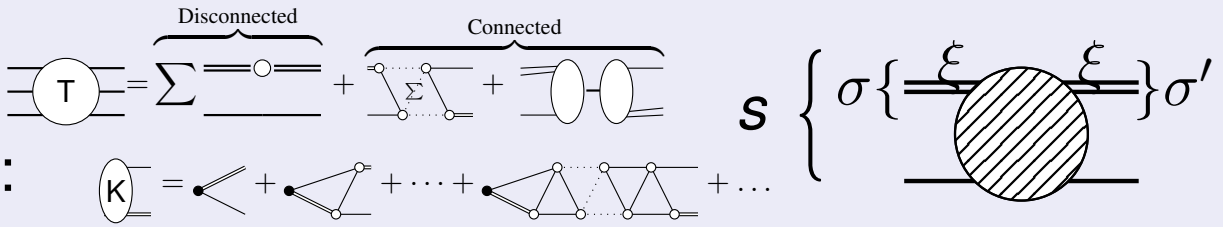


$$T(\sigma', s, \sigma) = K_\xi(s, \sigma') t(s) K_\xi(s, \sigma)$$

# Quasi-two-body unitarity

[MM (JPAC) in preparation]

## **Three-body** unitarity

[Eden, Landshoff et al.(2002)]

- Singularity splitting:
- Final state interaction:

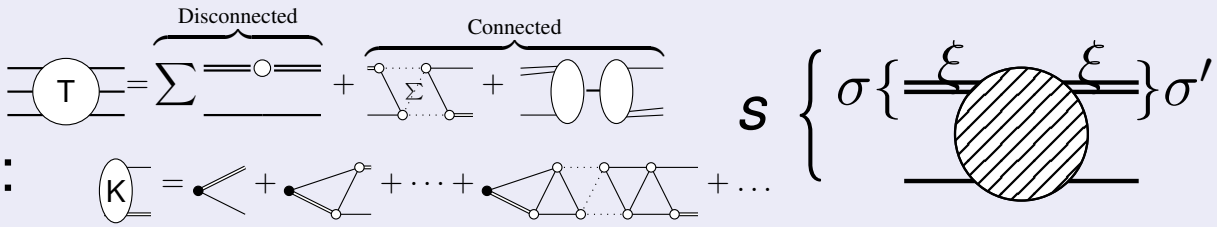


$$T(\sigma', s, \sigma) = K_\xi(s, \sigma') t(s) K_\xi(s, \sigma) \qquad 2\mathrm{Im}\, t(s) = t^*(s)\, \rho(s)\, t(s),$$

## Symmetrized quasi-two-body phase space factor

$$\rho(s) = \frac{1}{2} \int \mathrm{d}\Phi_3 \left| \quad - \quad \right|^2 = \int \mathrm{d}\Phi_3 \left[ \quad - \quad \right]$$

interference

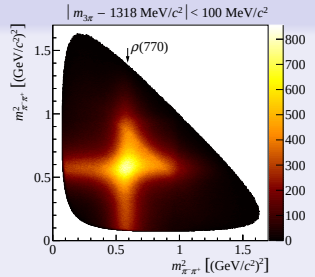

# Quasi-two-body unitarity

[MM (JPAC) in preparation]

## **Three-body** unitarity

[Eden, Landshoff et al.(2002)]

- Singularity splitting:
- Final state interaction:

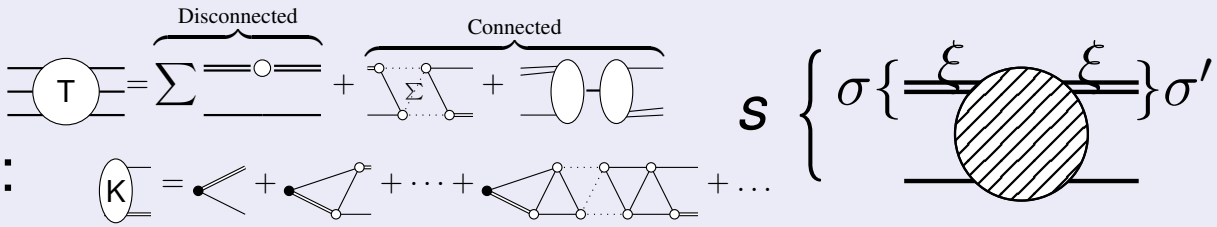


$$T(\sigma', s, \sigma) = K_\xi(s, \sigma') t(s) K_\xi(s, \sigma) \qquad 2\mathrm{Im}\, t(s) = t^*(s)\, \rho(s)\, t(s),$$

## Symmetrized quasi-two-body phase space factor

$$\rho(s) = \frac{1}{2} \int \mathrm{d}\Phi_3 \left| \quad - \quad \right|^2 = \int \mathrm{d}\Phi_3 \left[ \quad - \quad \right]$$

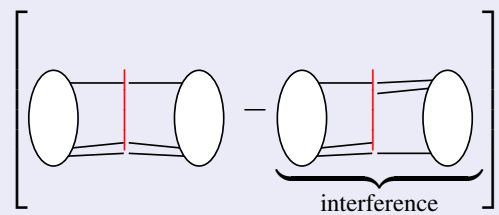


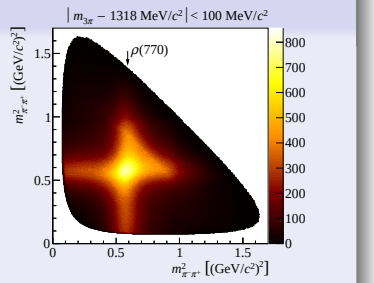


## The model: symmetrized

[Bowler, Phys.Lett.B182 (1986)]

$$t(s) = \frac{g^2}{m^2 - s - ig^2\rho(s)/2}$$

# Quasi-two-body unitarity

[MM (JPAC) in preparation]

## **Three-body** unitarity

[Eden, Landshoff et al.(2002)]

- Singularity splitting:
- Final state interaction:

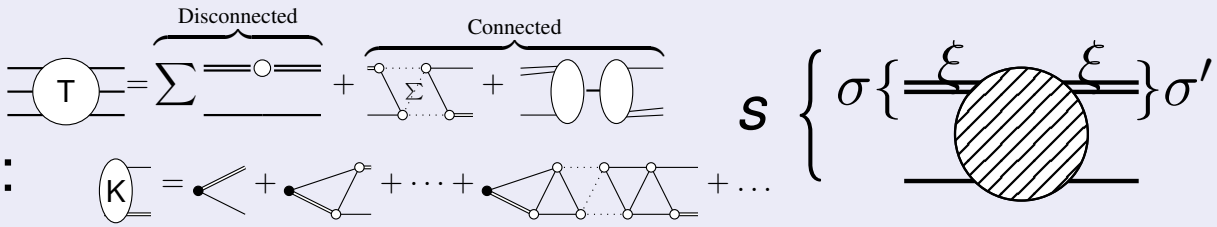


$$T(\sigma', s, \sigma) = K_\xi(s, \sigma')\, t(s)\, K_\xi(s, \sigma) \qquad 2\mathrm{Im}\, t(s) = t^*(s)\, \rho(s)\, t(s),$$

## Symmetrized quasi-two-body phase space factor

$$\rho(s) = \frac{1}{2}\int \mathrm{d}\Phi_3 \left| \quad - \quad \right|^2 = \int \mathrm{d}\Phi_3 \left[ \quad - \quad \right]$$



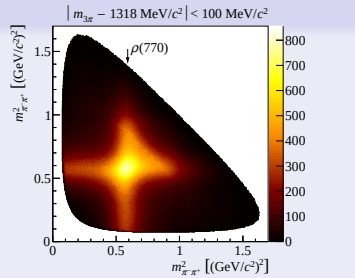


## The model: symmetrized, dispersive

$$t(s) = \frac{g^2}{m^2 - s - ig^2\tilde{\rho}(s)/2}, \qquad \tilde{\rho}(s) = \frac{s}{\pi i}\int_{9m_\pi^2}^{\infty} \frac{\rho(s')}{s'(s'-s)}\mathrm{d}s', \qquad \mathrm{Im}\, i\tilde{\rho} = i\rho.$$

# $1^{++}$ light meson spectrum

## Axial vector states below 2 GeV

- Dominated by $3\pi$ scattering
  - $\rho\pi \sim 60\% - 80\%$
  - $\sigma\pi \sim 5\% - 10\%$
  - $f_2\pi \sim < 5\%$
- $K\bar{K}\pi < 3\%$

# $1^{++}$ light meson spectrum

## Axial vector states below 2 GeV

- Dominated by $3\pi$ scattering
  - $\rho\pi \sim 60\% - 80\%$
  - $\sigma\pi \sim 5\% - 10\%$
  - $f_2\pi \sim < 5\%$
- $K\bar{K}\pi < 3\%$

## $\tau^- \to \pi^-\pi^+\pi^-\,\nu$

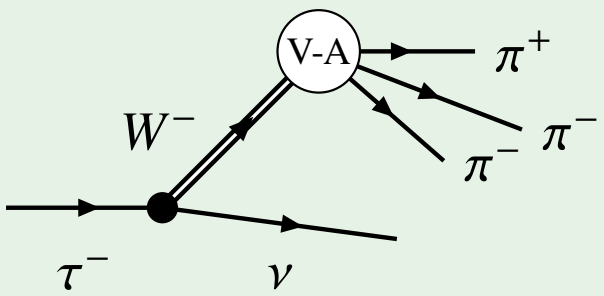


- V-A: Vector ($1^{--}$) or Axial ($1^{++}$)
- Isospin 1 due to the charge
- Negative $G$-parity $\Rightarrow$ positive $C$-parity

$\Rightarrow J^{PC} = 1^{++}$

# Fit to ALEPH data

[data from ALEPH, Phys.Rept.421 (2005)]

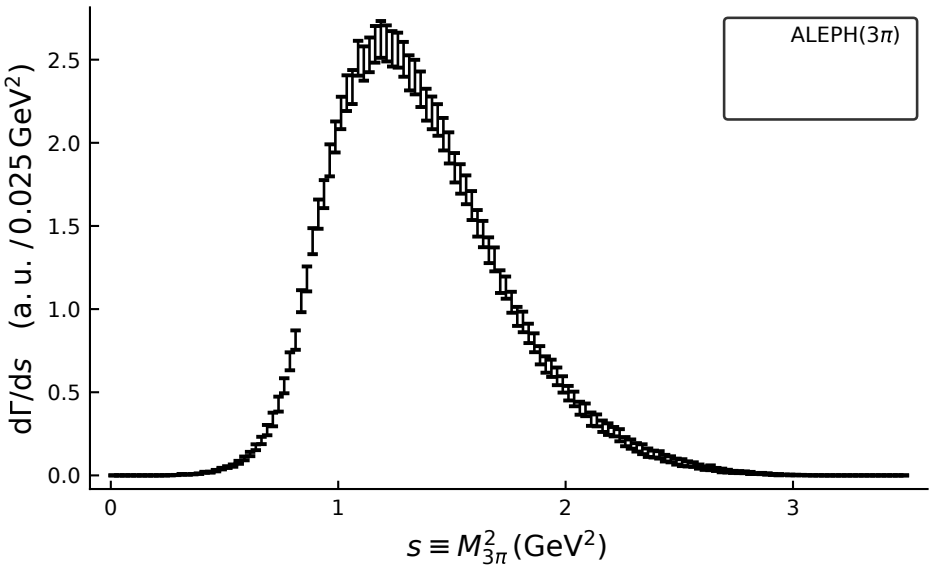


## $\chi^2$ function

$$\chi^2(c, m, g) = (\vec{D} - \vec{M}(c, m, g))^T C_{\text{stat}}^{-1} (\vec{D} - \vec{M}(c, m, g)),$$

- Stat. errors $\sim \times 5$ Systematic errors
- Stat. cov. matrix is used in the fit
- Syst. cov. matrix – in the bootstrap

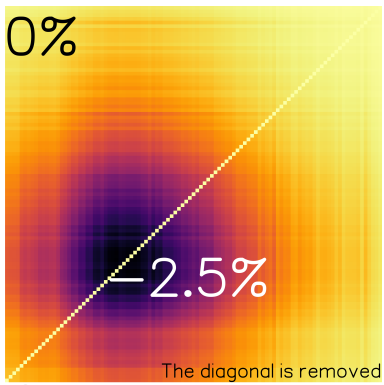


Stat. cov. matrix

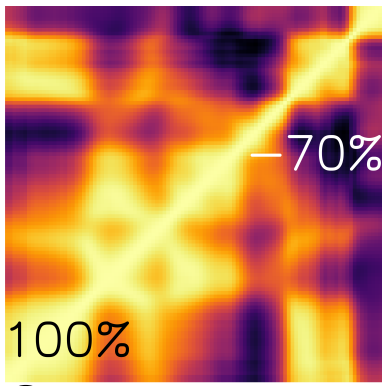


Syst. cov. matrix

# Fit to ALEPH data

[data from ALEPH, Phys.Rept.421 (2005)]

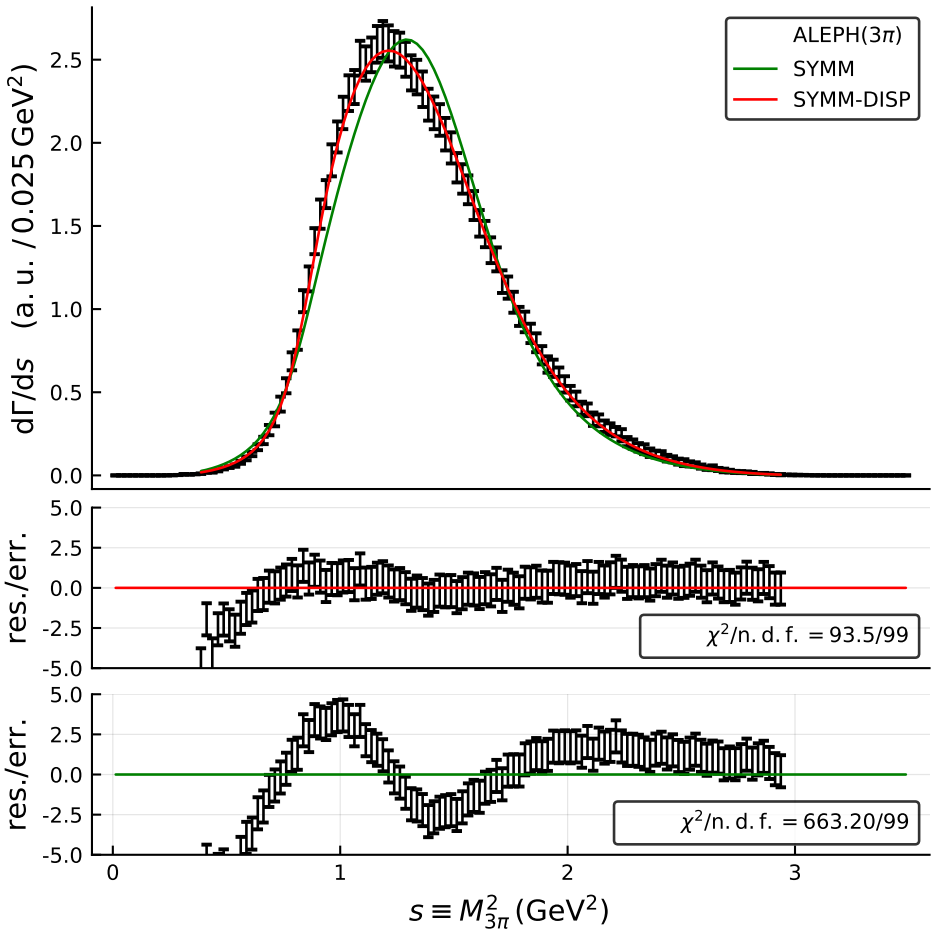


## $\chi^2$ function

$$\chi^2(c, m, g) = (\vec{D} - \vec{M}(c, m, g))^T C_{\text{stat}}^{-1} (\vec{D} - \vec{M}(c, m, g)),$$

- Stat. errors $\sim \times 5$ Systematic errors
- Stat. cov. matrix is used in the fit
- Syst. cov. matrix – in the bootstrap

# Fit to ALEPH data

[data from ALEPH, Phys.Rept.421 (2005)]

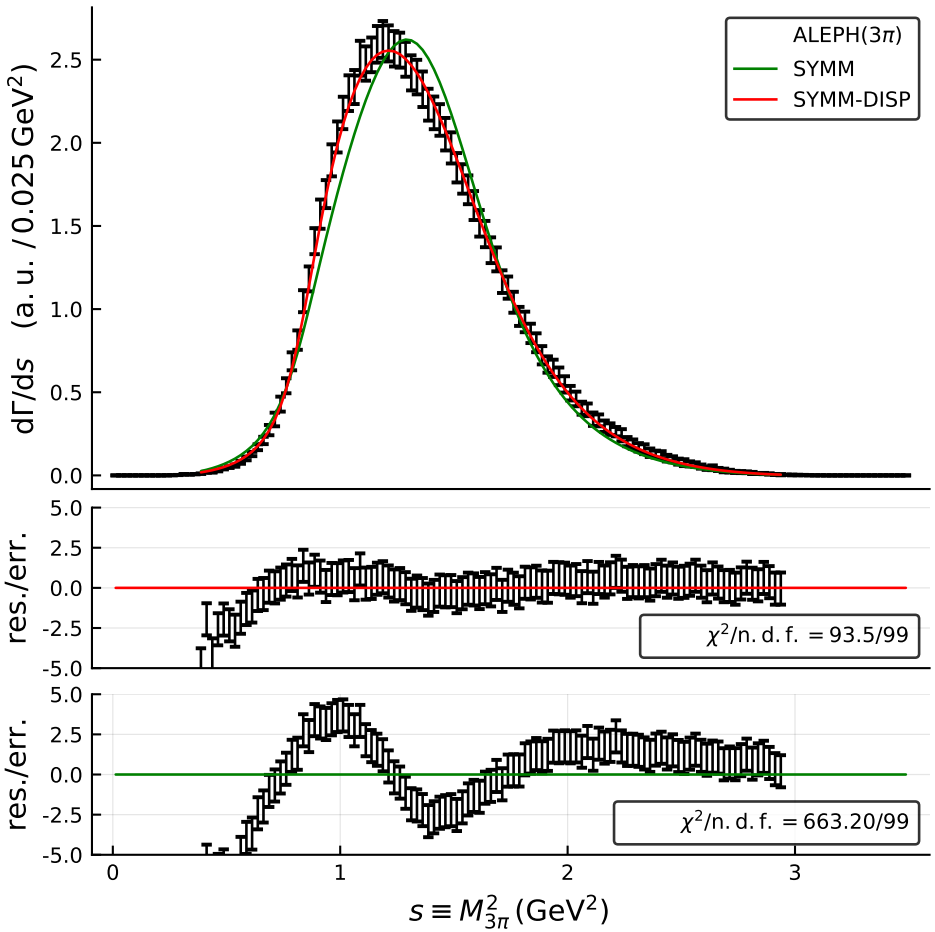


## $\chi^2$ function

$$\chi^2(c,m,g) = (\vec{D}-\vec{M}(c,m,g))^T C_{\text{stat}}^{-1}(\vec{D}-\vec{M}(c,m,g)),$$

- Stat. errors $\sim \times 5$ Systematic errors
- Stat. cov. matrix is used in the fit
- Syst. cov. matrix – in the bootstrap

## Breit-Wigner mass and width

- The BW mass is given by $\mathrm{Re}[t^{-1}(m^2)] = 0$
- The BW width $\Leftarrow \mathrm{Im}[g^2/t(m^2)] = m\Gamma_{\mathrm{BW}}$

Preliminary results:

$$m_{\mathrm{BW}}^{a_1(1260)} = (1.246 \pm 0.003)\,\mathrm{GeV},$$
$$\Gamma_{\mathrm{BW}}^{a_1(1260)} = (0.394 \pm 0.005)\,\mathrm{GeV}.$$

# Tour to the complex plane

## Analytical continuation

$$|t_{\ell}^{-1}(s)| = \left| \frac{m^2 - s}{g^2} - i \left( \frac{\tilde{\rho}(s)}{2} + \rho(s) \right) \right|.$$

- Analytical continuation of $\rho(s)$

$$\rho(s) \sim \int_{4m_\pi^2}^{(\sqrt{s}-m_\pi)^2} \frac{\mathrm{d}\sigma}{2\pi} U_\rho(\sigma) \frac{\lambda^{1/2}(s,\sigma,m_\pi^2)}{s}$$

- Error propagation using bootstrap analysis.

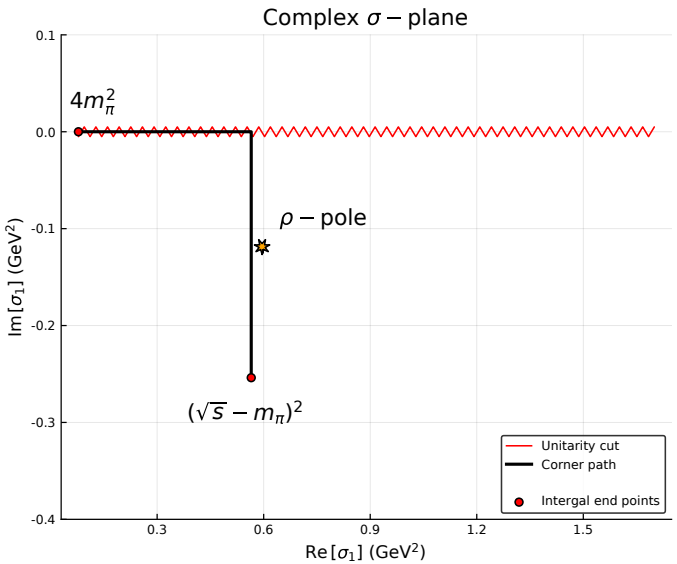

# Tour to the complex plane

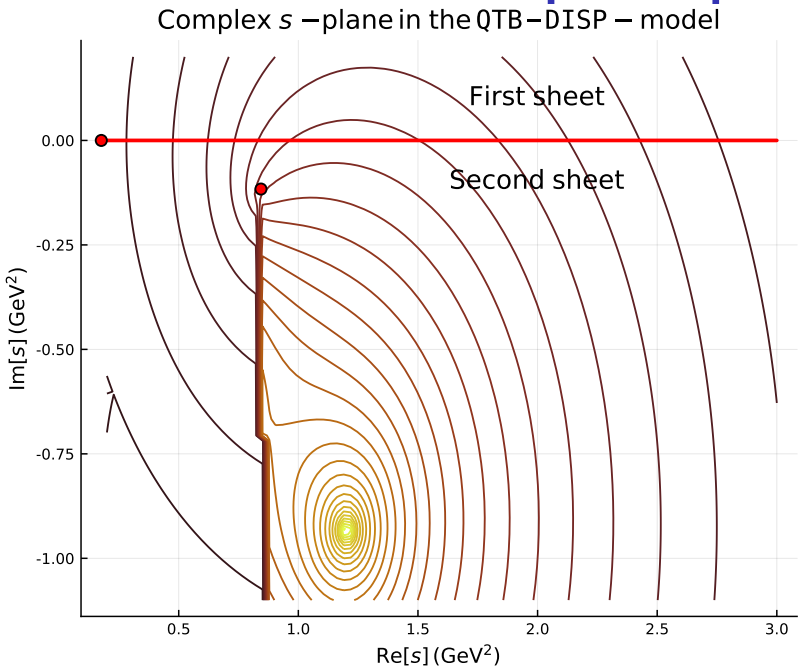


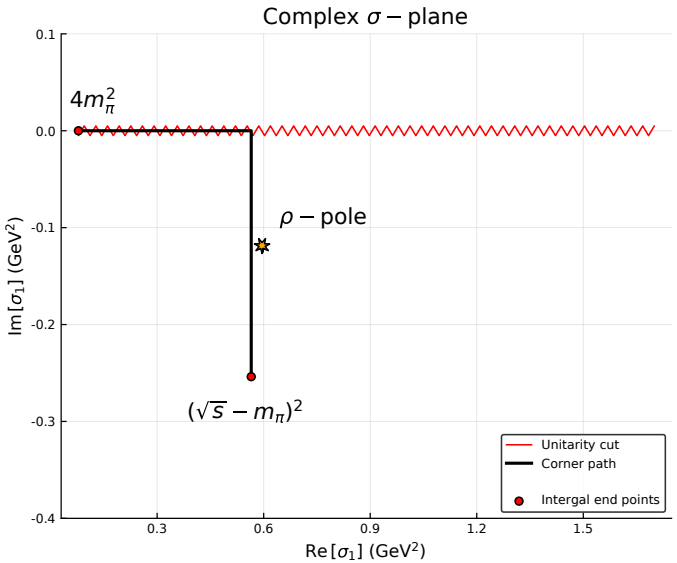


## Analytical continuation

$$|t_{\ell}^{-1}(s)| = \left| \frac{m^2 - s}{g^2} - i\left(\frac{\tilde{\rho}(s)}{2} + \rho(s)\right)\right|.$$

- Analytical continuation of $\rho(s)$

$$\rho(s) \sim \int_{4m_\pi^2}^{(\sqrt{s}-m_\pi)^2} \frac{\mathrm{d}\sigma}{2\pi} U_\rho(\sigma) \frac{\lambda^{1/2}(s,\sigma,m_\pi^2)}{s}$$

- Error propagation using bootstrap analysis.

# Tour to the complex plane

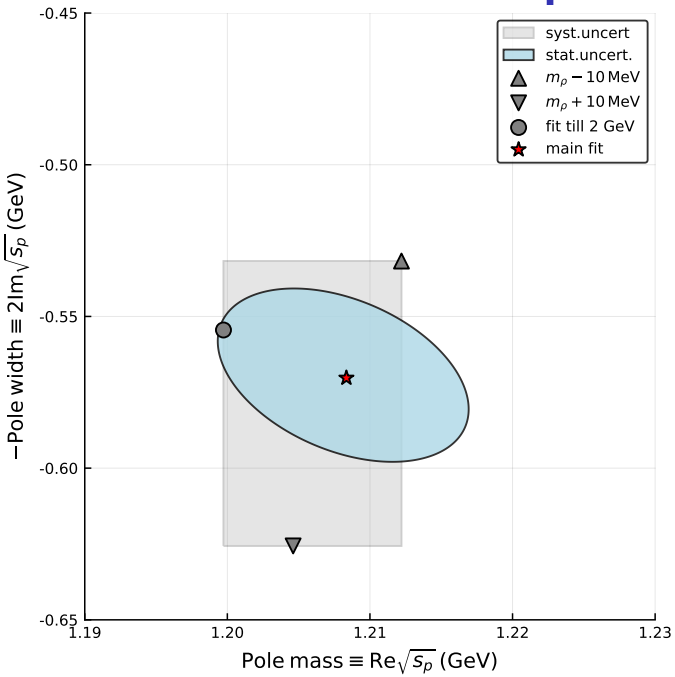


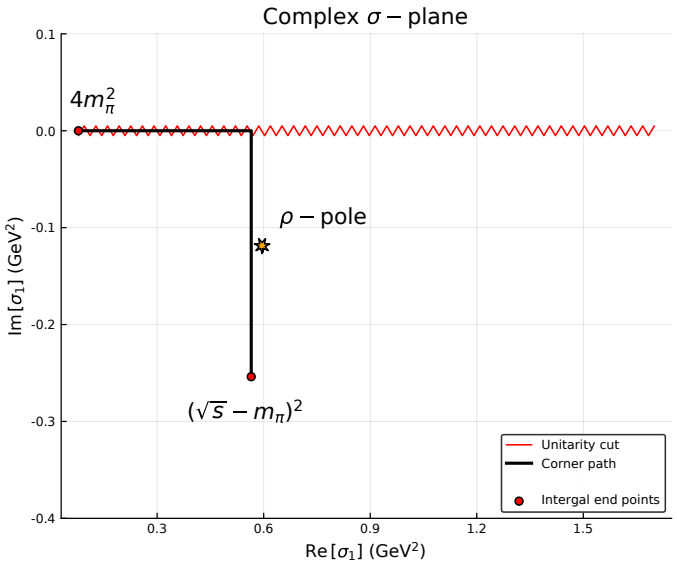


## Analytical continuation

$$|t_{\ell}^{-1}(s)| = \left| \frac{m^2 - s}{g^2} - i\left(\frac{\tilde{\rho}(s)}{2} + \rho(s)\right)\right|.$$

- Analytical continuation of $\rho(s)$

$$\rho(s) \sim \int_{4m_\pi^2}^{(\sqrt{s}-m_\pi)^2} \frac{\mathrm{d}\sigma}{2\pi} U_\rho(\sigma) \frac{\lambda^{1/2}(s,\sigma,m_\pi^2)}{s}$$

- Error propagation using bootstrap analysis.

## Prel. results for the pole position

$$m_p^{(a_1(1260))} = (1.208 \pm 0.004)\,\mathrm{GeV},$$
$$\Gamma_p^{(a_1(1260))} = (0.569 \pm 0.012)\,\mathrm{GeV}.$$

Systematic studies:

- variation of $\rho$-shape
- variation of fit range

# Tour to the complex plane

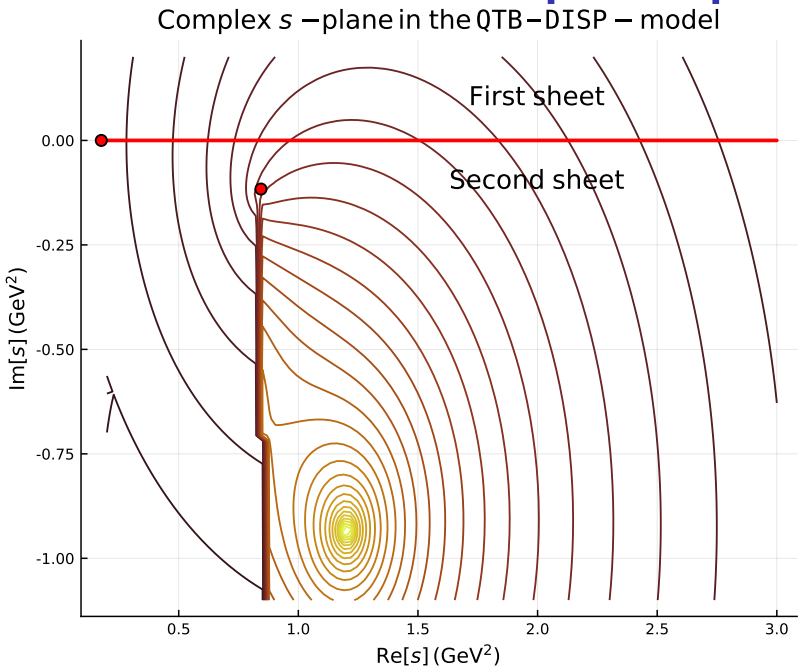


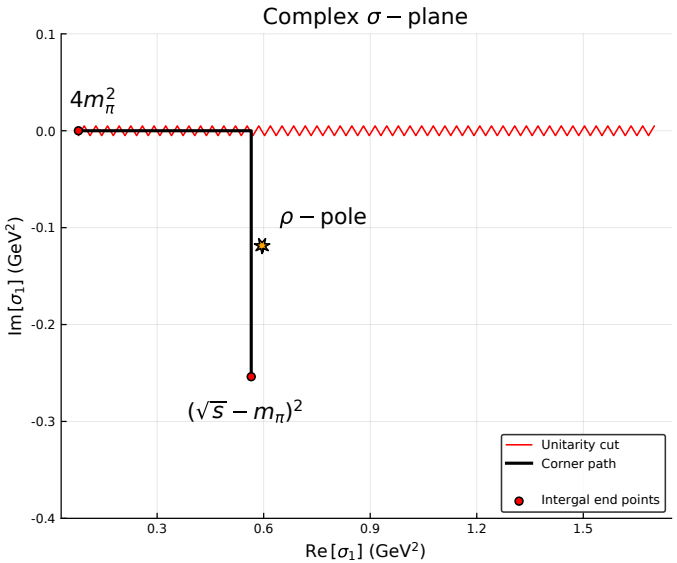


## Analytical continuation

$$|t_{\ell}^{-1}(s)| = \left| \frac{m^2 - s}{g^2} - i\left(\frac{\tilde{\rho}(s)}{2} + \rho(s)\right)\right|.$$

- Analytical continuation of $\rho(s)$

$$\rho(s) \sim \int_{4m_\pi^2}^{(\sqrt{s}-m_\pi)^2} \frac{\mathrm{d}\sigma}{2\pi} U_\rho(\sigma) \frac{\lambda^{1/2}(s,\sigma,m_\pi^2)}{s}$$

- Error propagation using bootstrap analysis.

## Prel. results for the pole position

$$m_p^{(a_1(1260))} = (1.208 \pm 0.004)\,\mathrm{GeV},$$
$$\Gamma_p^{(a_1(1260))} = (0.569 \pm 0.012)\,\mathrm{GeV}.$$

Systematic studies:

- variation of $\rho$-shape
- variation of fit range

# Tour to the complex plane

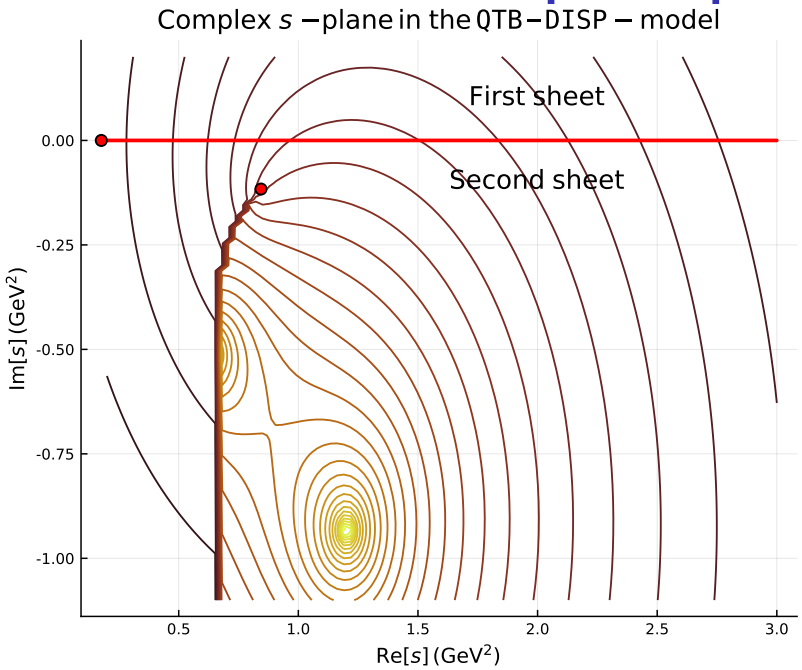


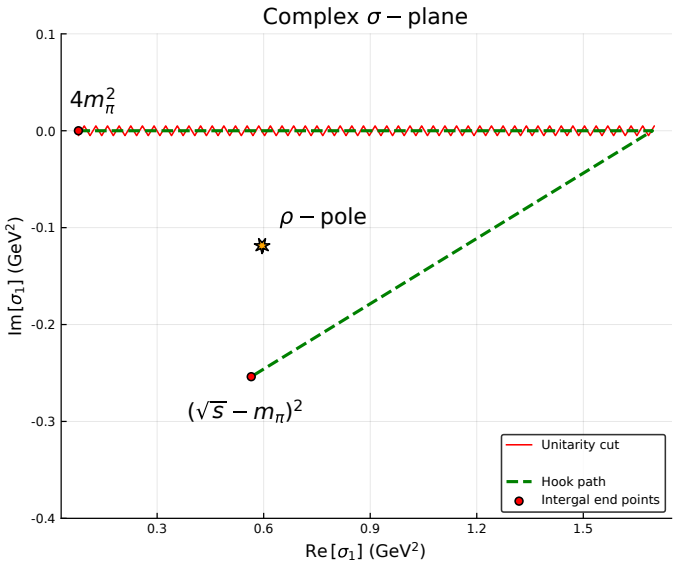


## Analytical continuation

$$|t_{\ell}^{-1}(s)| = \left| \frac{m^2 - s}{g^2} - i\left(\frac{\tilde{\rho}(s)}{2} + \rho(s)\right)\right|.$$

- Analytical continuation of $\rho(s)$

$$\rho(s) \sim \int_{4m_\pi^2}^{(\sqrt{s}-m_\pi)^2} \frac{\mathrm{d}\sigma}{2\pi} U_\rho(\sigma) \frac{\lambda^{1/2}(s,\sigma,m_\pi^2)}{s}$$

- Error propagation using bootstrap analysis.

## Prel. results for the pole position

$$m_p^{(a_1(1260))} = (1.208 \pm 0.004)\,\mathrm{GeV},$$
$$\Gamma_p^{(a_1(1260))} = (0.569 \pm 0.012)\,\mathrm{GeV}.$$

Systematic studies:

- variation of $\rho$-shape
- variation of fit range

# Tour to the complex plane

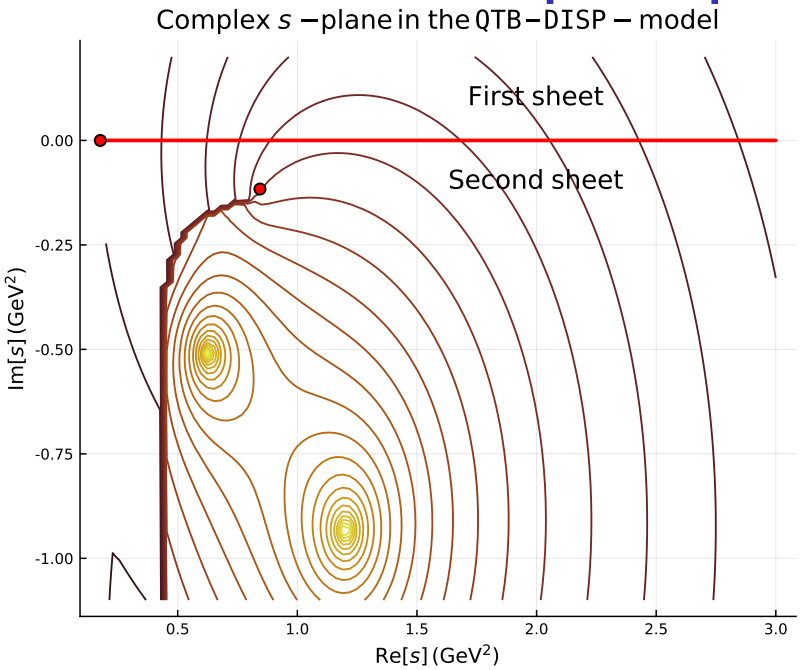


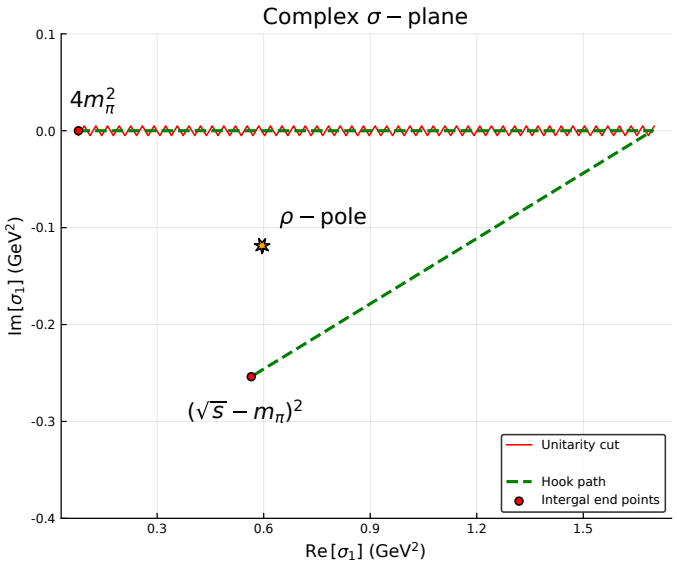


## Analytical continuation

$$|t_{\ell}^{-1}(s)| = \left| \frac{m^2 - s}{g^2} - i\left(\frac{\tilde{\rho}(s)}{2} + \rho(s)\right)\right|.$$

- Analytical continuation of $\rho(s)$

$$\rho(s) \sim \int_{4m_\pi^2}^{(\sqrt{s}-m_\pi)^2} \frac{\mathrm{d}\sigma}{2\pi} U_\rho(\sigma) \frac{\lambda^{1/2}(s,\sigma,m_\pi^2)}{s}$$

- Error propagation using bootstrap analysis.

## Prel. results for the pole position

$$m_p^{(a_1(1260))} = (1.208 \pm 0.004)\,\mathrm{GeV},$$
$$\Gamma_p^{(a_1(1260))} = (0.569 \pm 0.012)\,\mathrm{GeV}.$$

Systematic studies:

- variation of $\rho$-shape
- variation of fit range

# Tour to the complex plane

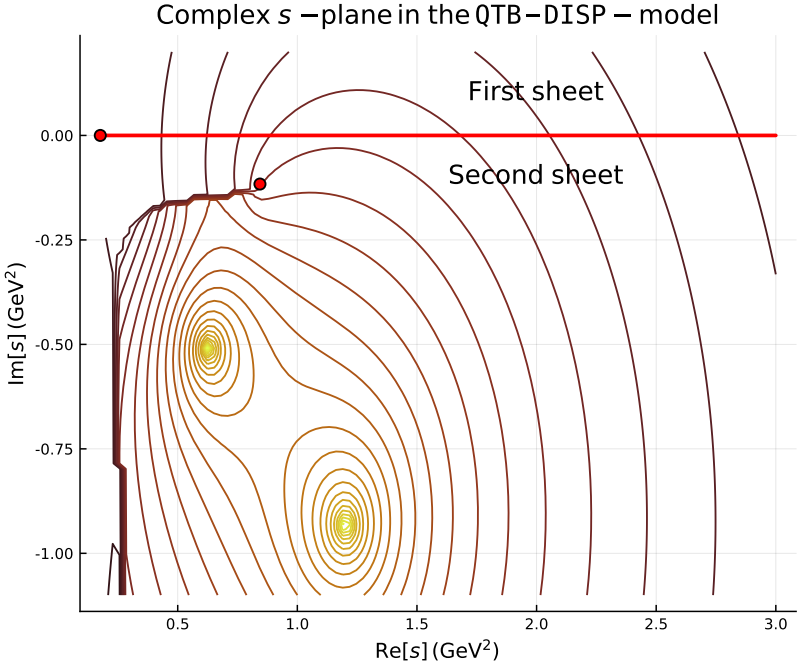


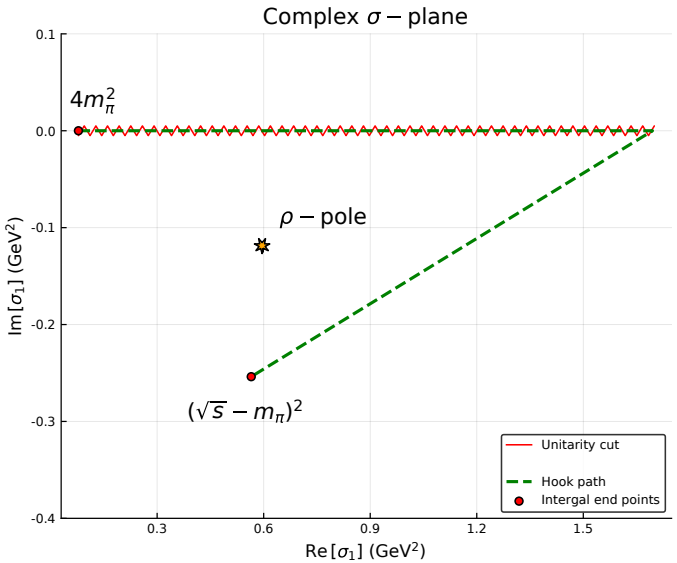


## Analytical continuation

$$|t_{\ell}^{-1}(s)| = \left| \frac{m^2 - s}{g^2} - i\left(\frac{\tilde{\rho}(s)}{2} + \rho(s)\right)\right|.$$

- Analytical continuation of $\rho(s)$

$$\rho(s) \sim \int_{4m_\pi^2}^{(\sqrt{s}-m_\pi)^2} \frac{\mathrm{d}\sigma}{2\pi} U_\rho(\sigma) \frac{\lambda^{1/2}(s,\sigma,m_\pi^2)}{s}$$

- Error propagation using bootstrap analysis.

## Prel. results for the pole position

$$m_p^{(a_1(1260))} = (1.208 \pm 0.004)\,\mathrm{GeV},$$
$$\Gamma_p^{(a_1(1260))} = (0.569 \pm 0.012)\,\mathrm{GeV}.$$

Systematic studies:

- variation of $\rho$-shape
- variation of fit range

# The spurious pole

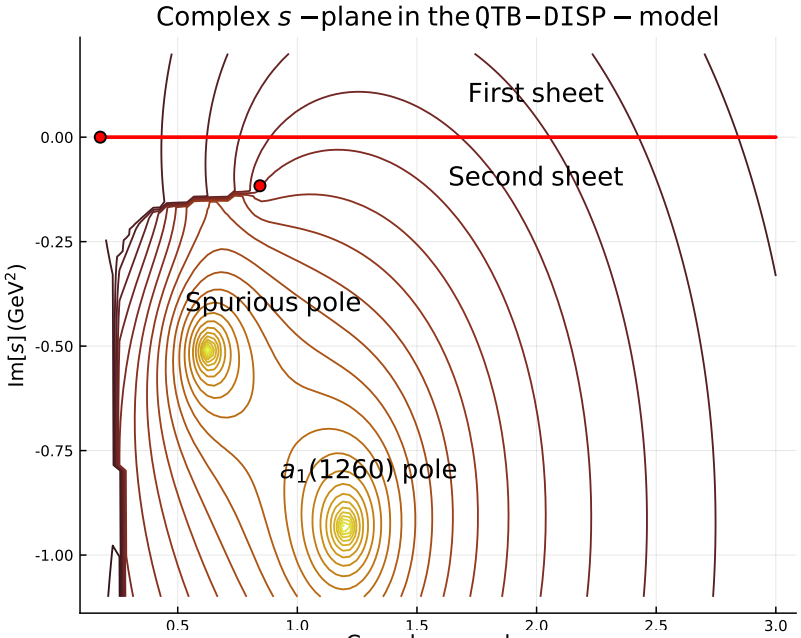


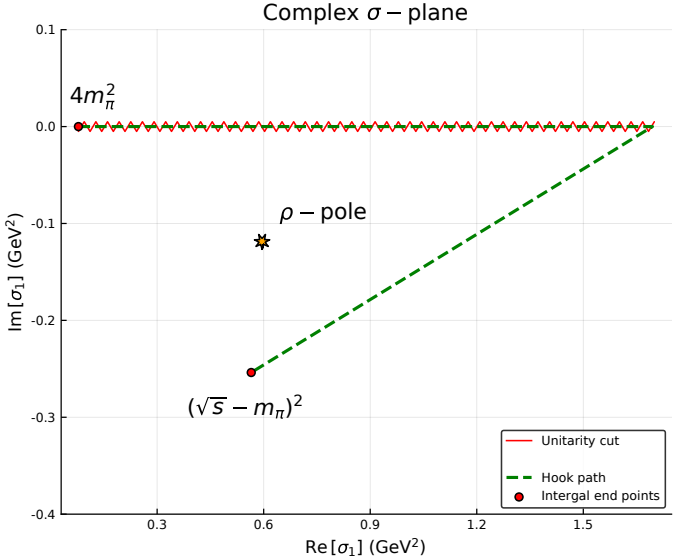


## The reason of the spurious pole

$$\rho(s) \sim \int_{4m_\pi^2}^{(\sqrt{s}-m_\pi)^2} \frac{d\sigma}{2\pi} U_\rho(\sigma) \frac{\lambda^{1/2}(s,\sigma,m_\pi^2)}{s}$$

- Not every pole is the resonance

# The spurious pole

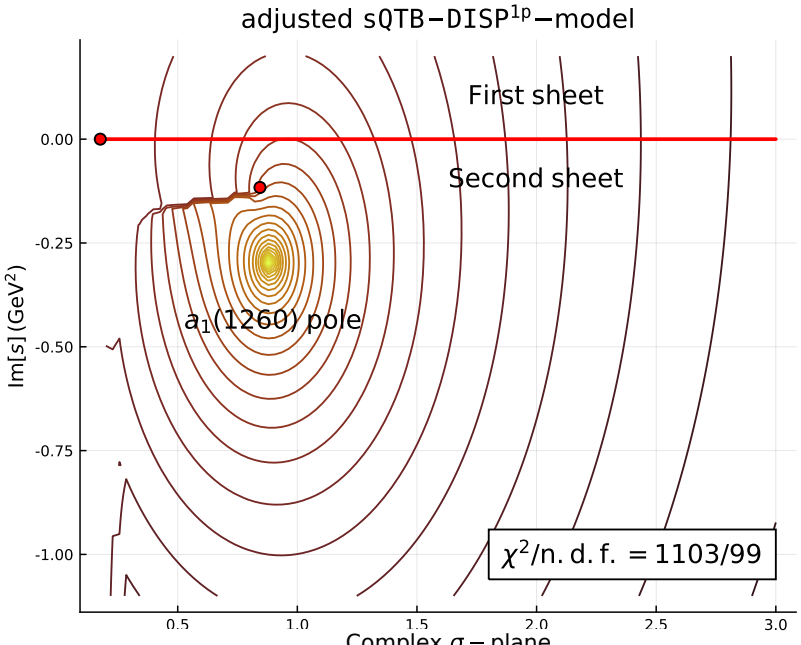


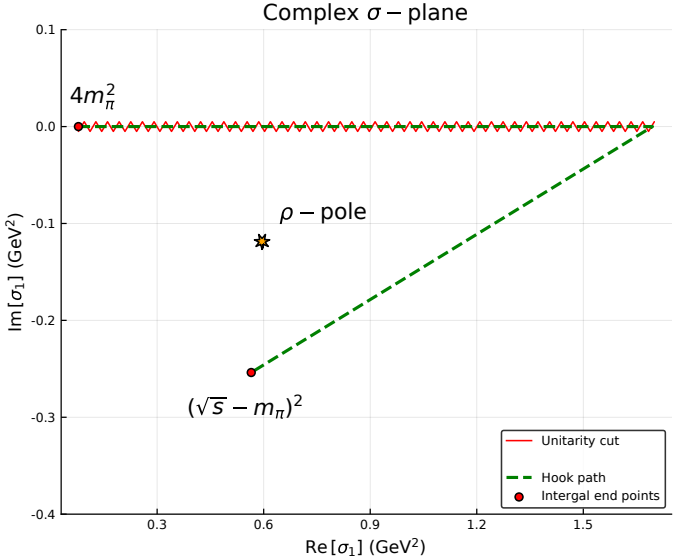


## The reason of the spurious pole

$$\rho(s) \sim \int_{4m_\pi^2}^{(\sqrt{s}-m_\pi)^2} \frac{d\sigma}{2\pi} U_\rho(\sigma) \frac{\lambda^{1/2}(s,\sigma,m_\pi^2)}{s}$$

- Not every pole is the resonance

## Can we find the model without the pole

- Denoting $\hat{t}(s) = t(s)/s$

$$2\mathrm{Im}\,\hat{t}(s) = \hat{t}^*(s)\,(s\rho(s))\,\hat{t}(s),$$

- New model

$$c/(P_k(s) - ig^2 s\hat{\rho}(s)/2)$$

$P_1(s) = m^2 - s$ does not fit the data

# The spurious pole

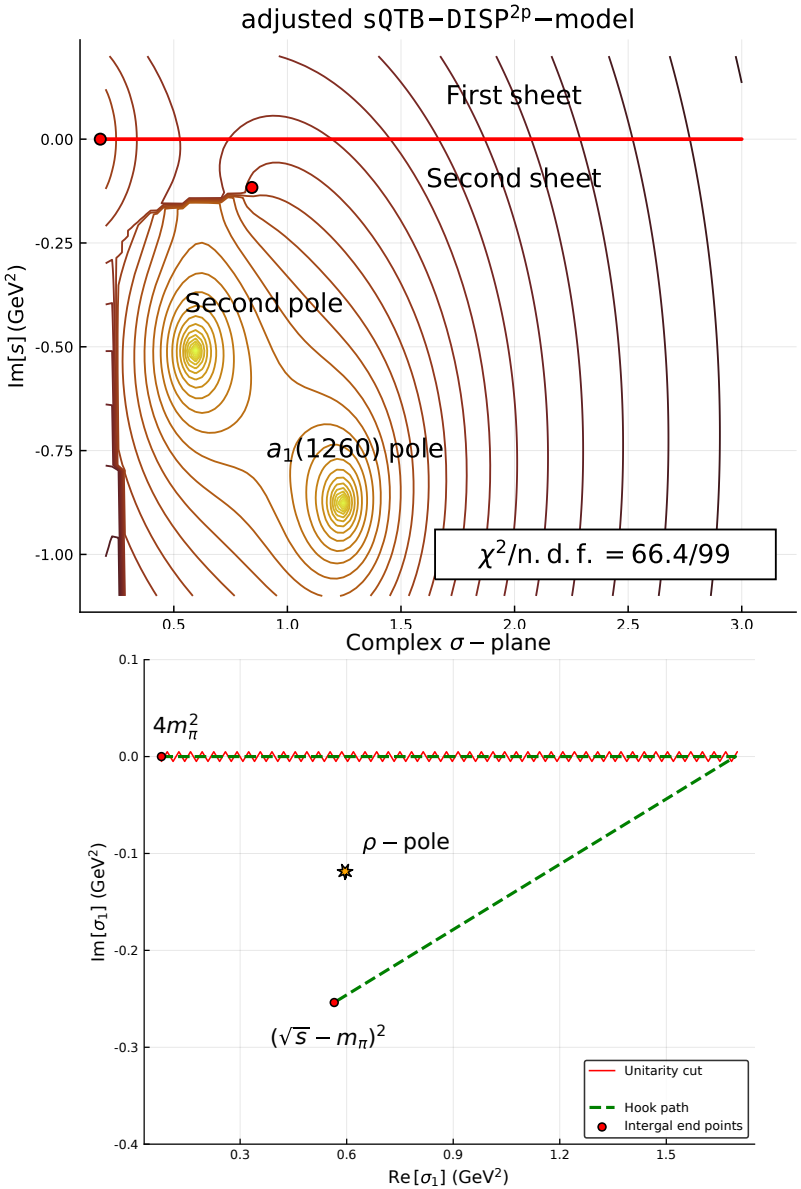


## The reason of the spurious pole

$$\rho(s) \sim \int_{4m_\pi^2}^{(\sqrt{s}-m_\pi)^2} \frac{d\sigma}{2\pi} U_\rho(\sigma) \frac{\lambda^{1/2}(s,\sigma,m_\pi^2)}{s}$$

- Not every pole is the resonance

## Can we find the model without the pole

- Denoting $\hat{t}(s) = t(s)/s$

$$2\mathrm{Im}\,\hat{t}(s) = \hat{t}^*(s)\,(s\rho(s))\,\hat{t}(s),$$

- New model

$$c/(P_k(s) - ig^2 s\hat{\rho}(s)/2)$$

$P_1(s) = m^2 - s$ does not fit the data

$P_2(s) = s(m^2 - s) + h$ gives a good fit and the same pole

# Summary

- Three-body unitarity is important for hadron spectroscopy
  - both experimental and lattice
  - The light $1^{++}$ sector is the first place to study it
- We found a class of models which can satisfy unitarity exactly:
  - Factorization and final state interaction.
- Free parameters are constrained using ALEPH data (where is Belle, BES data !?).
- Analytical continuation:
  - requires an accurate integral path deformation.
  - The pole of the $a_1(1260)$ resonance was found.

## The spurious pole

- The dynamics in the channel requires strong influence of the left singularities (the threshold region is important).
- Systematic studies are ongoing.

Thank you for the attention

Thanks to

B. Ketzer, COMPASS colleagues,
A. Jackura, A. Pilloni, A. Szczepaniak (JPAC)

# EXTRA MATERIAL

# $1^{++}$ interaction in scattering experiments

## $a_1(1260)$ at COMPASS

[COMPASS, PRD 95 (2017)]

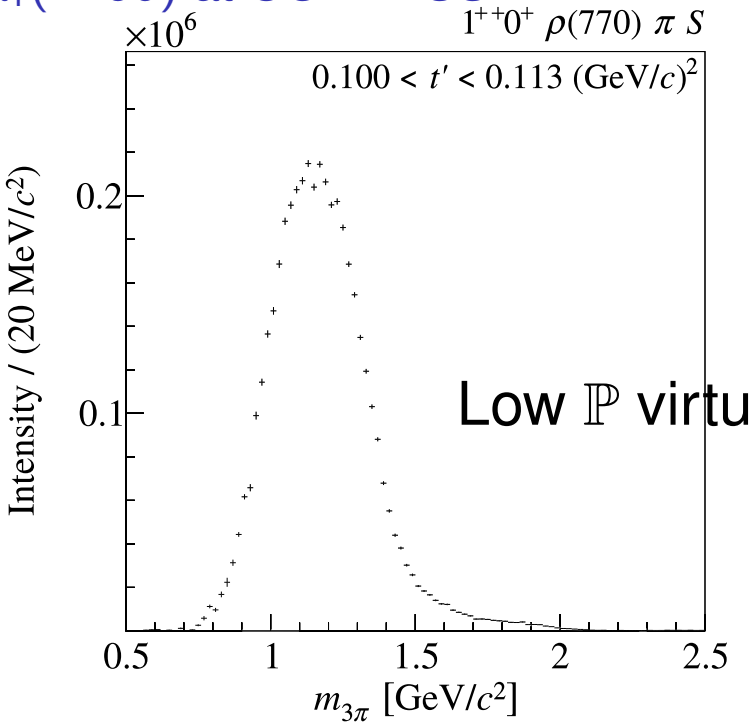


Low $\mathbb{P}$ virtuality

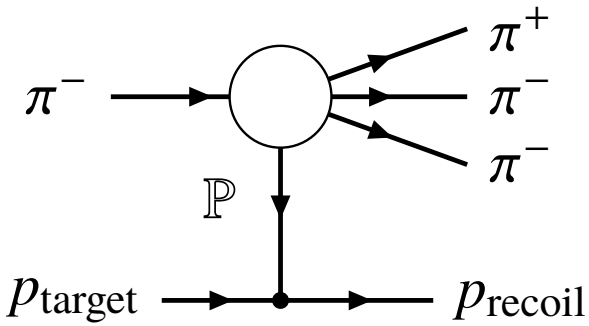

# $1^{++}$ interaction in scattering experiments

## $a_1(1260)$ at COMPASS

[COMPASS, PRD 95 (2017)]

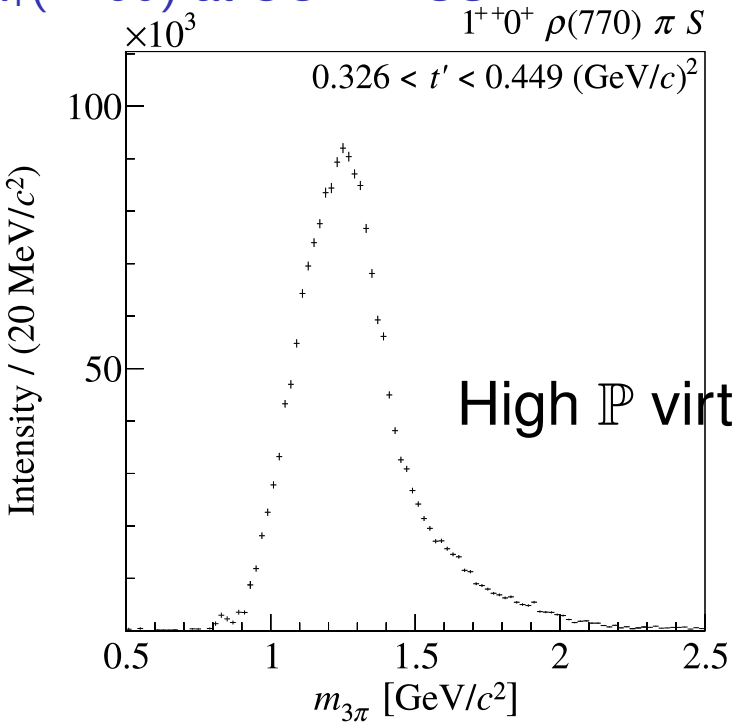


High $\mathbb{P}$ virtuality

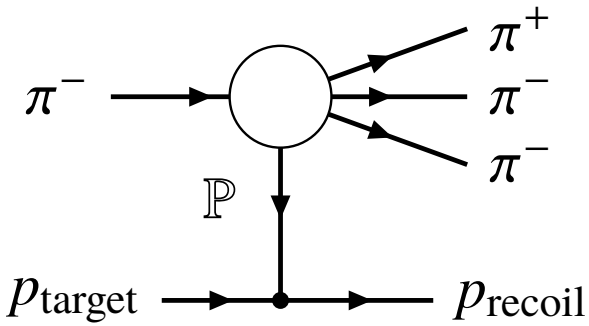

# $1^{++}$ interaction in scattering experiments

## $a_1(1260)$ at COMPASS

[COMPASS, PRD 95 (2017)]

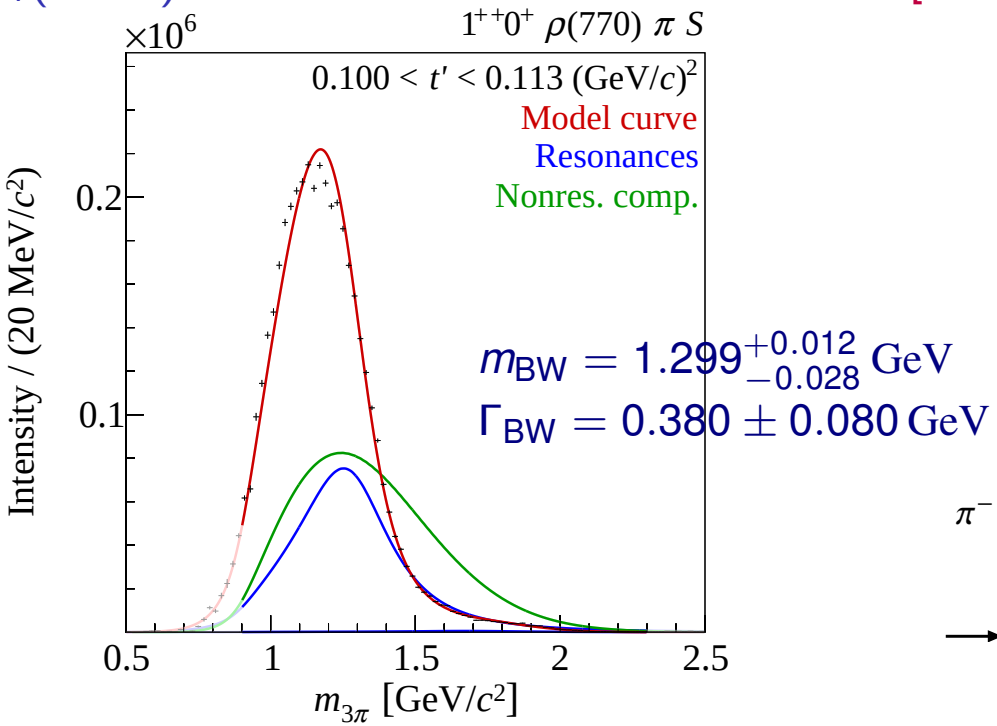


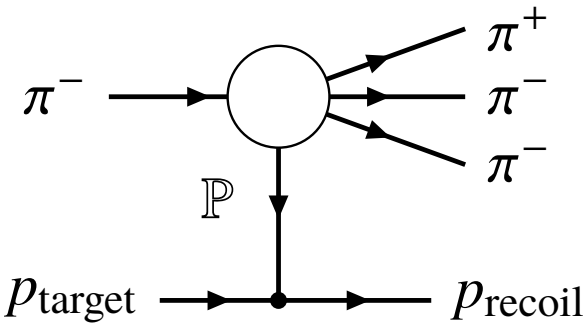


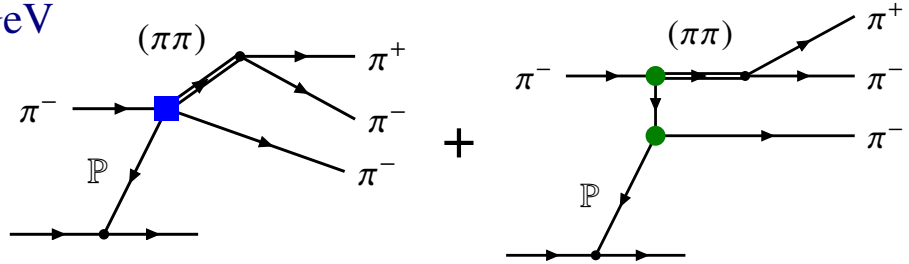


## COMPASS Model

- Partial wave analysis to isolate $1^{++}$ sector.
- Coherent addition of the short and the long range diagrams $\Rightarrow$ (no unitarity)

# $1^{++}$ interaction in scattering experiments

## $a_1(1260)$ at COMPASS

[COMPASS, PRD 95 (2017)]

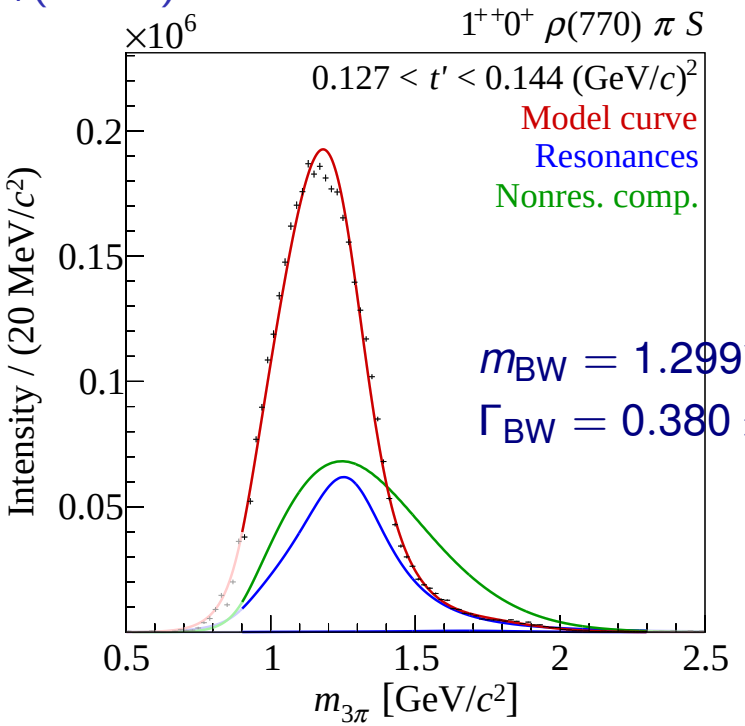


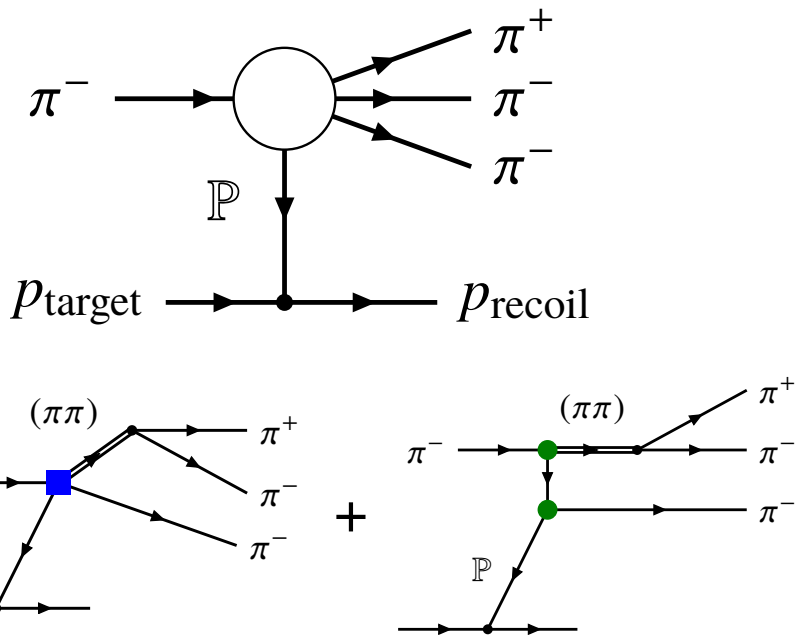


## COMPASS Model

- Partial wave analysis to isolate $1^{++}$ sector.
- Coherent addition of the short and the long range diagrams $\Rightarrow$ (no unitarity)

# $1^{++}$ interaction in scattering experiments

## $a_1(1260)$ at COMPASS

[COMPASS, PRD 95 (2017)]

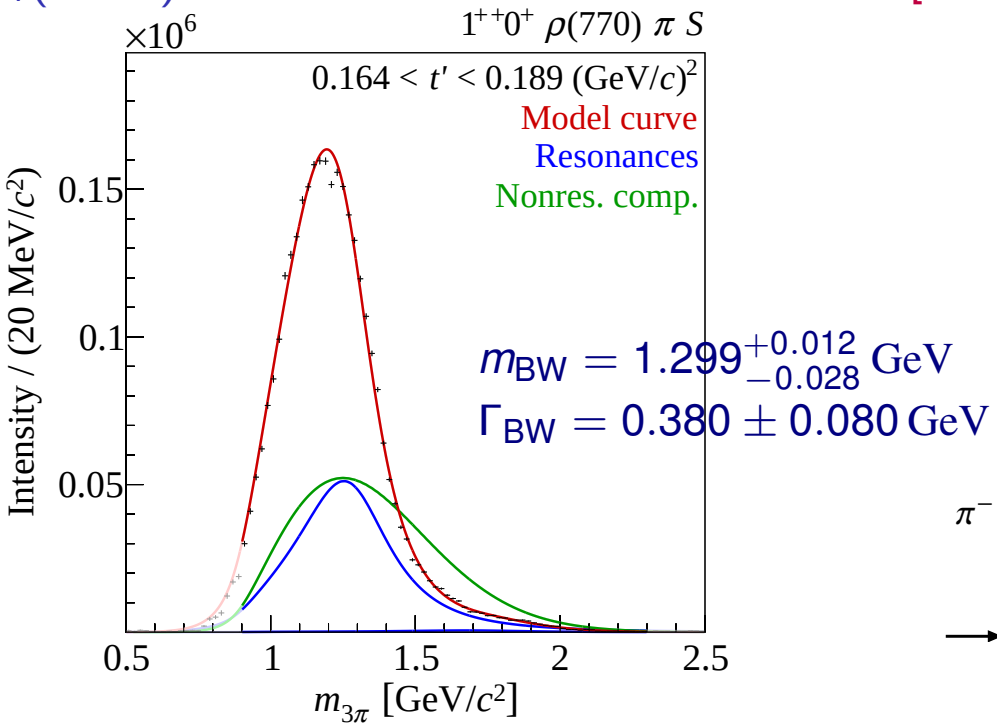


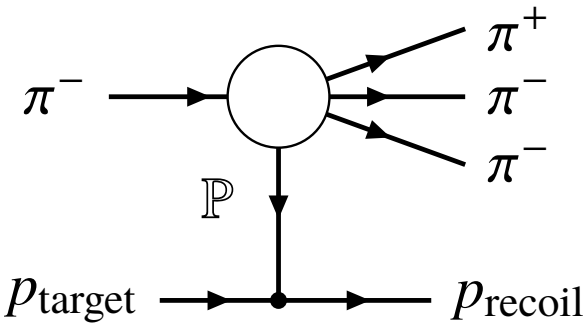


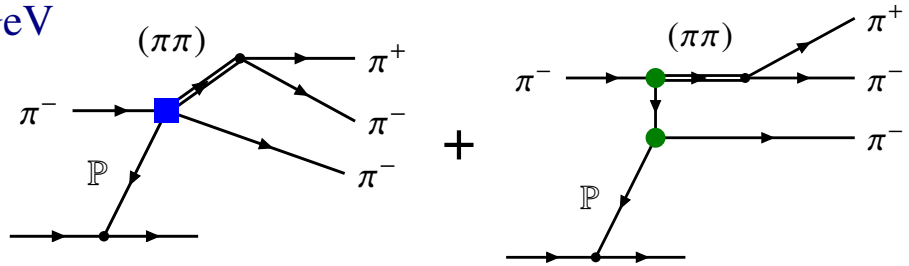


## COMPASS Model

- Partial wave analysis to isolate $1^{++}$ sector.
- Coherent addition of the short and the long range diagrams $\Rightarrow$ (no unitarity)

# $1^{++}$ interaction in scattering experiments

## $a_1(1260)$ at COMPASS

[COMPASS, PRD 95 (2017)]

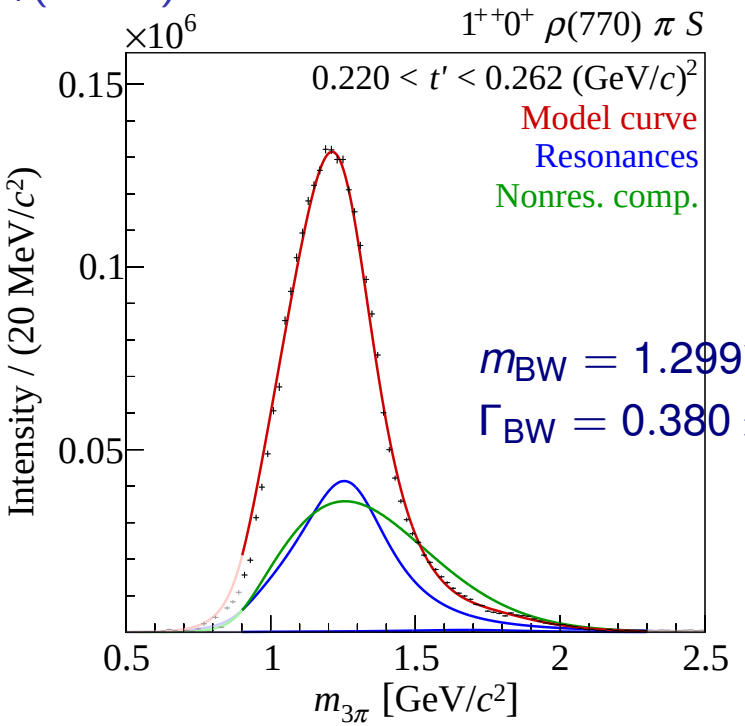


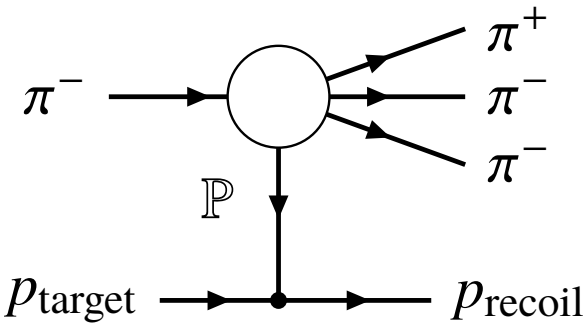


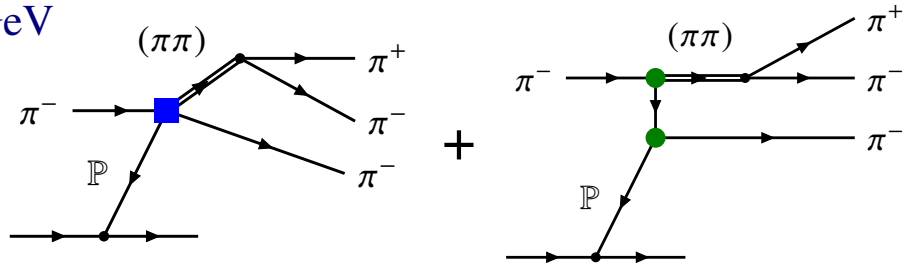


## COMPASS Model

- Partial wave analysis to isolate $1^{++}$ sector.
- Coherent addition of the short and the long range diagrams $\Rightarrow$ (no unitarity)

# $1^{++}$ interaction in scattering experiments

## $a_1(1260)$ at COMPASS

[COMPASS, PRD 95 (2017)]

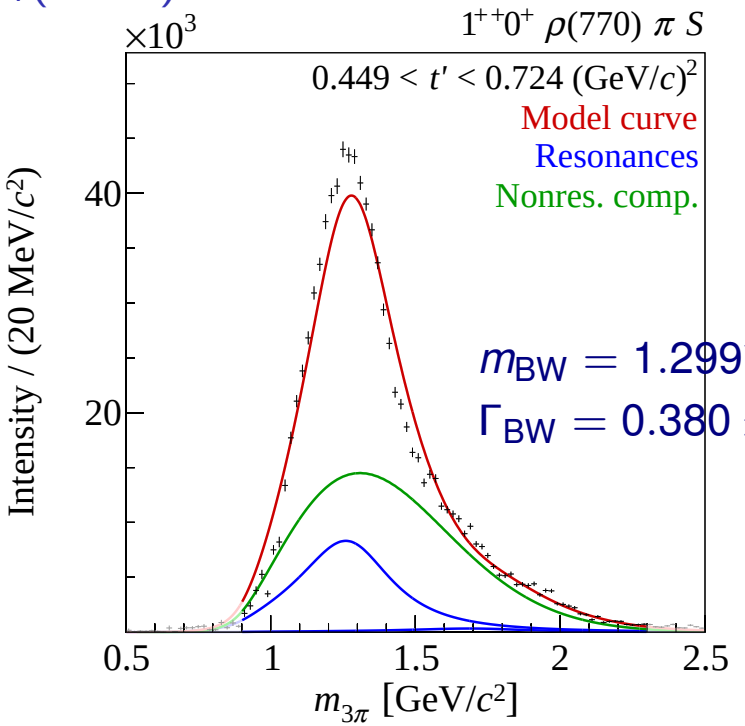


$$m_{\mathrm{BW}} = 1.299^{+0.012}_{-0.028}\ \mathrm{GeV}$$

$$\Gamma_{\mathrm{BW}} = 0.380 \pm 0.080\ \mathrm{GeV}$$

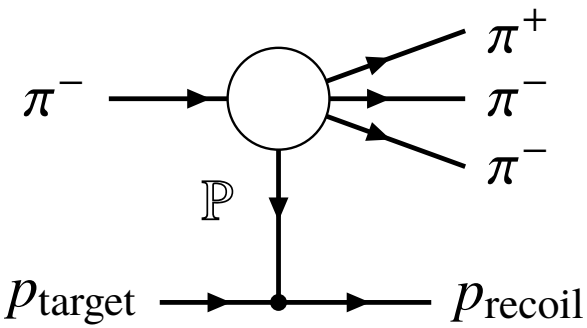


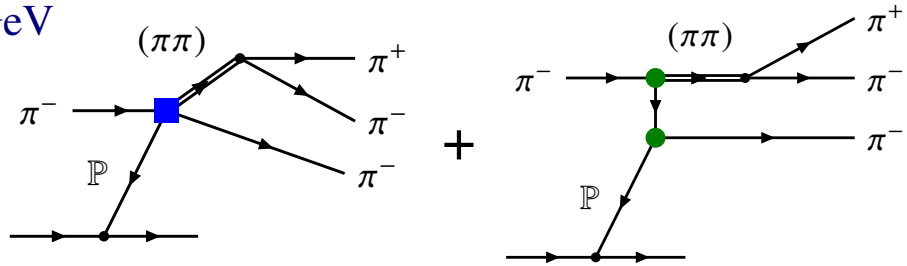


## COMPASS Model

- Partial wave analysis to isolate $1^{++}$ sector.
- Coherent addition of the short and the long range diagrams $\Rightarrow$ (no unitarity)

# $3\pi$ at CLEO, [Phys.Rev. D61 (2000) 012002]

Partial wave analysis:

- combined fit with 7 waves.
- 5 isobars $\rho$, $\rho(1450)$, $f_2(1270)$, $\sigma$, $f_0(1370)$.
- significant contribution of $K^*\bar{K}$

## Main fit results

- $m_{a_1} \approx 1.33\,\text{GeV}$, $\Gamma_{a_1}(m_{a_1}) \approx 0.814\,\text{GeV}$,
- Branching fractions:
  - $\text{Br}(a_1 \to \rho\pi) \approx 60\%$,
  - $\text{Br}(a_1 \to \sigma\pi) \approx 20\%$,
  - $\text{Br}(a_1 \to f_0(1370)\pi) \approx 7\%$,
  - $\text{Br}(a_1 \to K^*\bar{K}) \approx 2.2\%$.

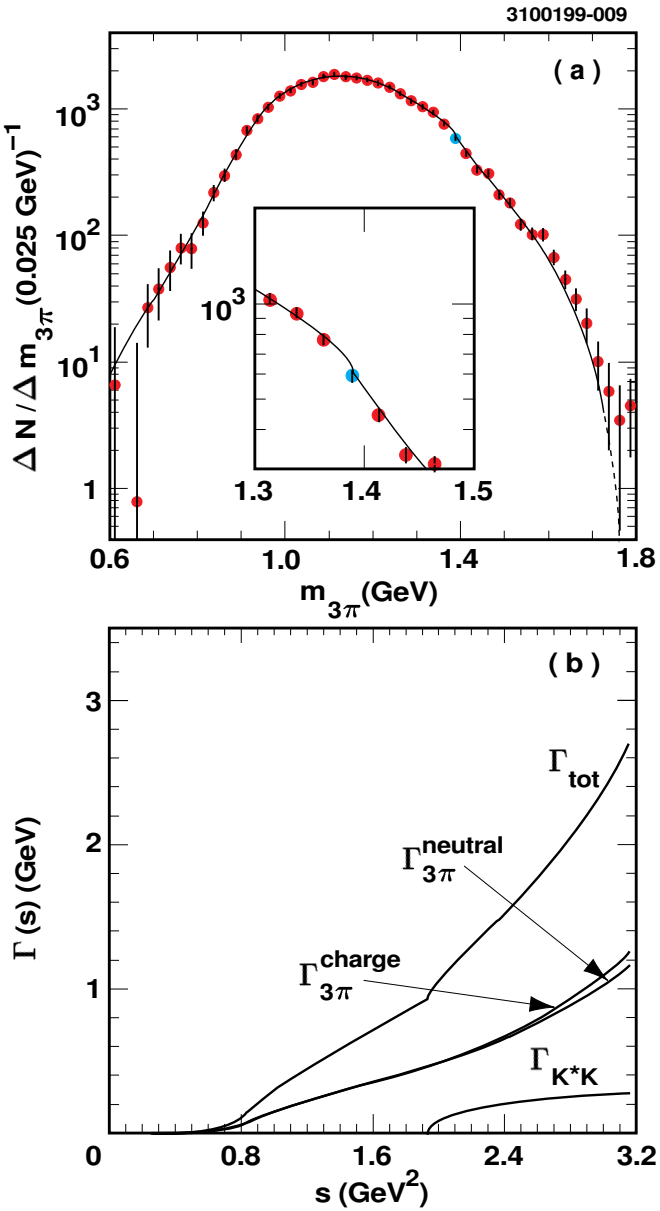

# $J^{PC} = 1^{++}$ sector

[PRL 115 (2015) 082001]

## $a_1(1420)$ phenomenon

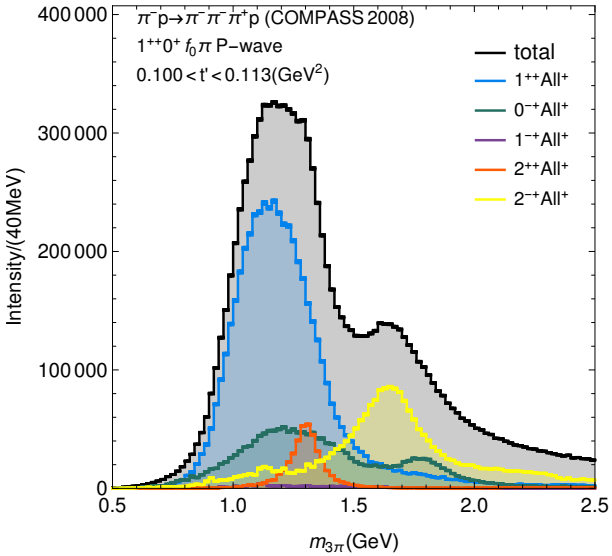

# $J^{PC} = 1^{++}$ sector

[PRL 115 (2015) 082001]

## $a_1(1420)$ phenomenon

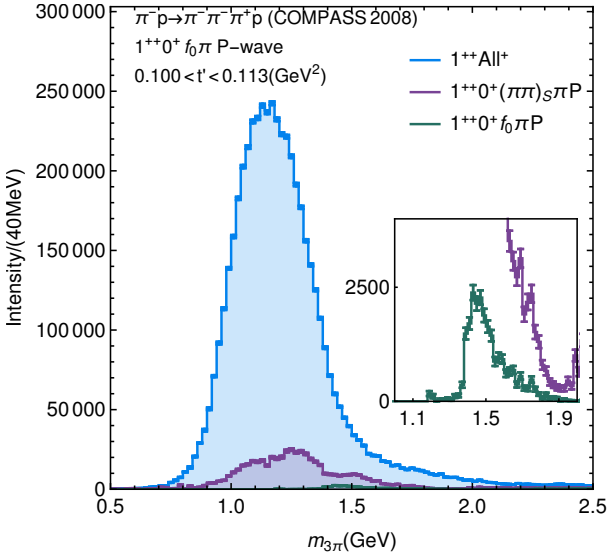

# $J^{PC} = 1^{++}$ sector

[PRL 115 (2015) 082001]

## $a_1(1420)$ phenomenon

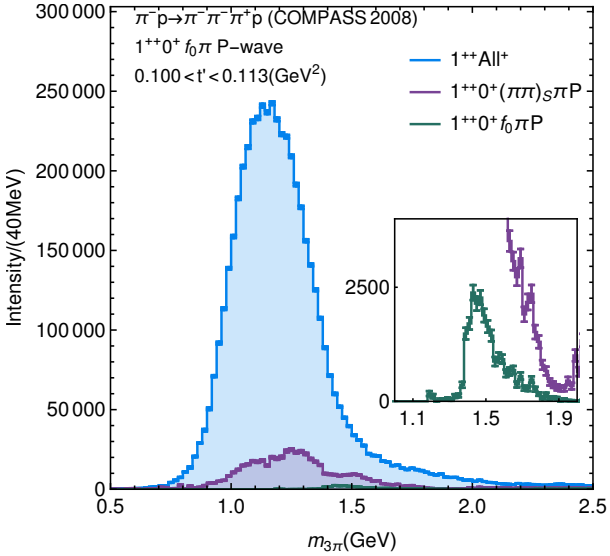


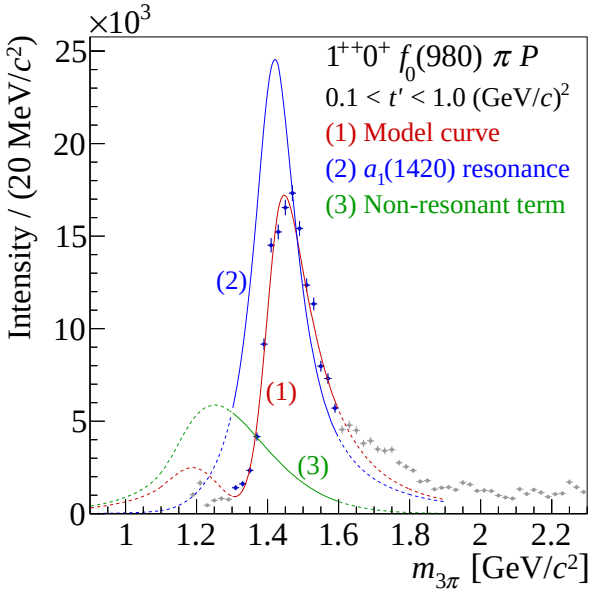


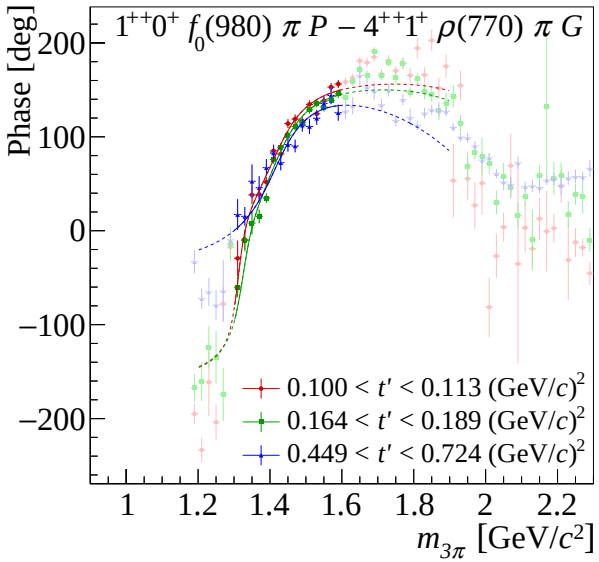

# $J^{PC} = 1^{++}$ sector

[PRL 115 (2015) 082001]

## $a_1(1420)$ phenomenon

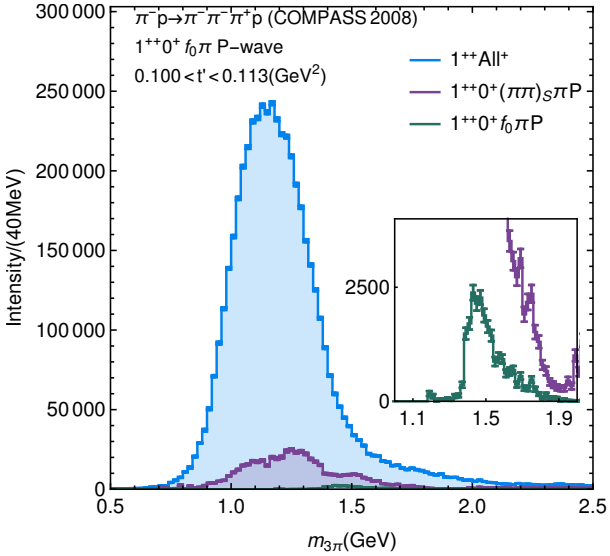


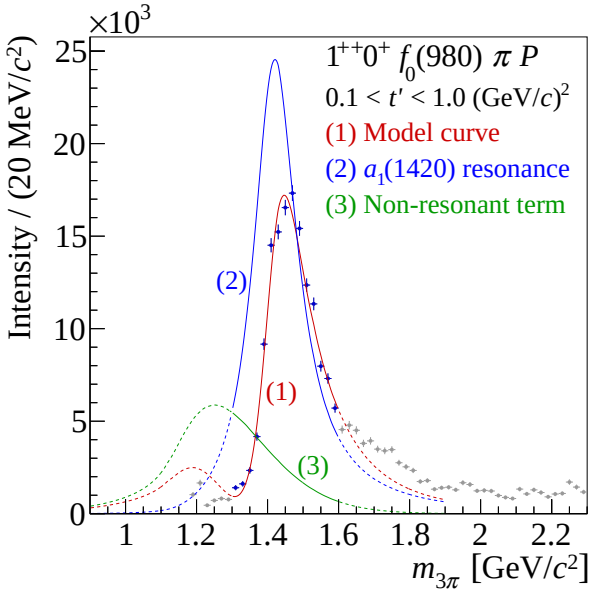


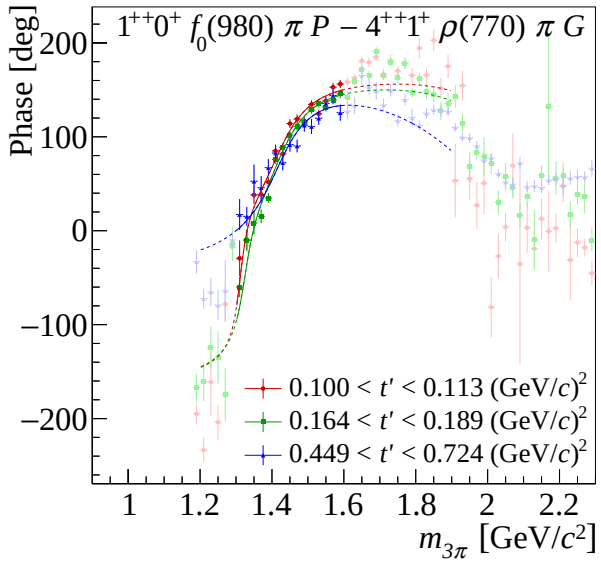



## Not something ordinary

- Does not fit to the radial excitation trajectory
- Too close to ground state $a_1(1260)$
- Width narrower than ground state
- Mass is very close to the $K^*\bar{K}$ thereshold

# Selection of $a_1(1420)$

## Enhancement in COMPASS data $\pi\, p \to 3\pi\, p$

3π Dalitz plot, {1.4 GeV < $M_{3\pi}$ < 1.5 GeV}

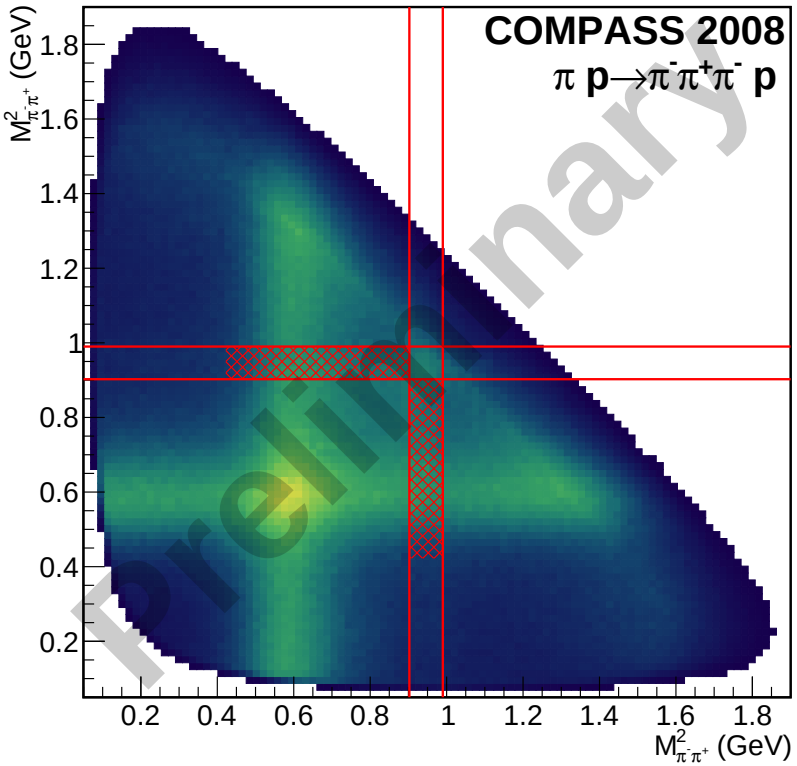


"$f_0$-band-cut" in the Dalitz plot

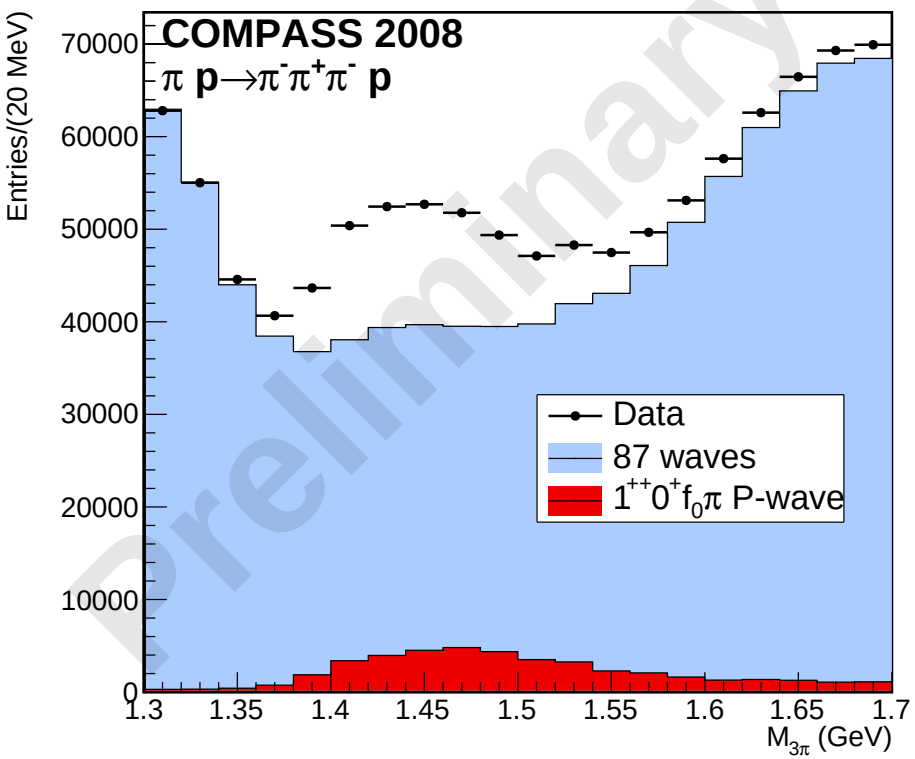


- A simple cut on the Dalitz plot ($f_0$ band) enhances bump in $M_{3\pi}$
- Partial wave analysis proves that the origin is the $a_1(1420)$.